Universidad Zaragoza
1542

Trabajo Fin de Máster
Máster en Ingeniería Biomédica

Cellular response due to substrate stiffness variations: A phenomenological model

Autor

Aarón Xerach Herrera Martín

Directores

José Manuel García Aznar
Carlos Borau Zamora

Departamento de Ingeniería Mecánica
Escuela de Ingeniería y Arquitectura
Universidad de Zaragoza

Septiembre 2013

Universidad Zaragoza
1542

Cellular response due to substrate stiffness variations: A phenomenological model

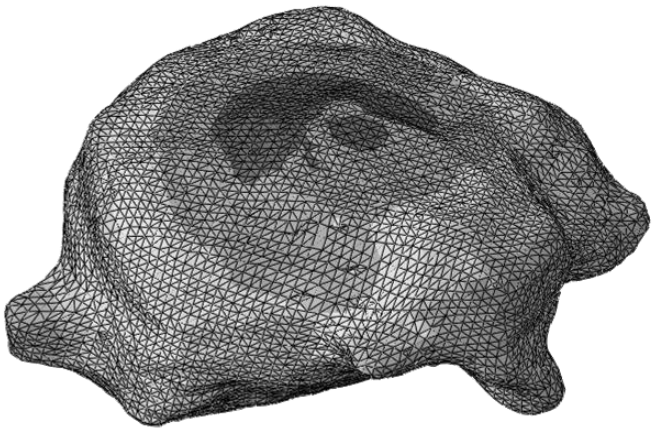

Appendix I – Calculation report

Appendix I - Calculation report

1. Introduction.

In this section are exposed the whole results obtained during the development of the work. The main results are included and commented in the Main Report.

2. Checking the model.

The first step before start the calculations is checking the model with simplified geometry and boundary conditions. The cubic geometry, composed of eight C3D8 elements, has symmetric like boundary conditions. Therefore, there is no force applied, allowing the geometry to contract freely.

Taking into account the expressions developed in the Main Report, the force exerted by the cell can be written as follows:

$$\sigma_{cell,ij} = -\frac{\theta_{max}}{\varepsilon_{min}}\varepsilon_{c,ii} + \theta_{max} + K_{pas}\varepsilon_{cell,ij} \tag{2.1}$$

knowing that $\varepsilon_c = \varepsilon_{cell} - \varepsilon_{act}$ and rearranging the expression, it is obtained the equation below:

$$\sigma_{cell,ij} = \frac{K_{act}\,\theta_{max}}{K_{act}\,\varepsilon_{min} - \theta_{max}}\left(\varepsilon_{min} - \varepsilon_{cell,ij}\right) + K_{pas}\varepsilon_{cell,ij} \tag{2.2}$$

Since there is no force in this model, the value of ε_{cell} can be obtained from the expression above, corresponding its value to ε_{cell} = -0.3174. This result is in agreement with the obtained in the computational model showed in figure I.1.

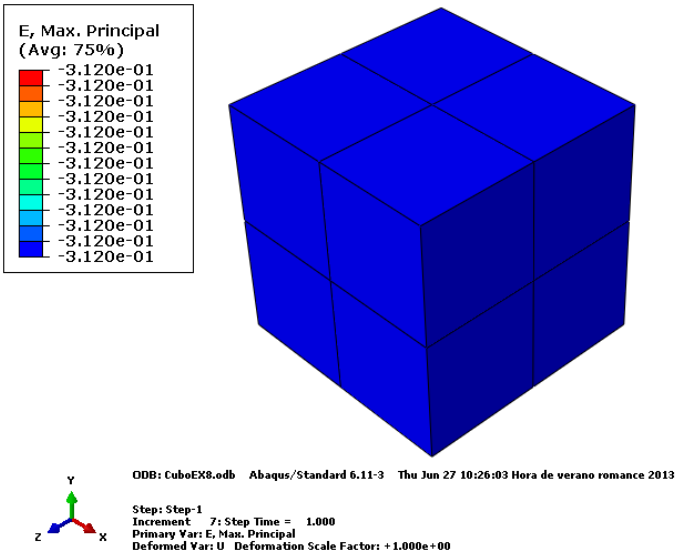

Figure I.1. Simplified model employed to check the behaviour equations. The result of the strain is in agreement with the theoretical value: 0.3120 versus 0.3174.

3. Modelling the Mitrossilis et al. experiment.

The developed model aims to reproduce the experiment of Mitrossilis et al. using the Finite Element Method. Thus, the model comprises three parts (Figure I.2 and I.3):

- Flexible top plate. It has 311.25 μm length, 100 μm width and it is discretized with 1240 S4 elements.

- Cell. It has 30 μm height and between 24 μm and 30 μm width depending on the cell shape: Cylinder like or barrel like. It is composed of 4560 C3D8 elements.

- Lower plate, modelled as a rigid solid with 100 R3D4 elements. It has enough surface to allow cell contraction and movement.

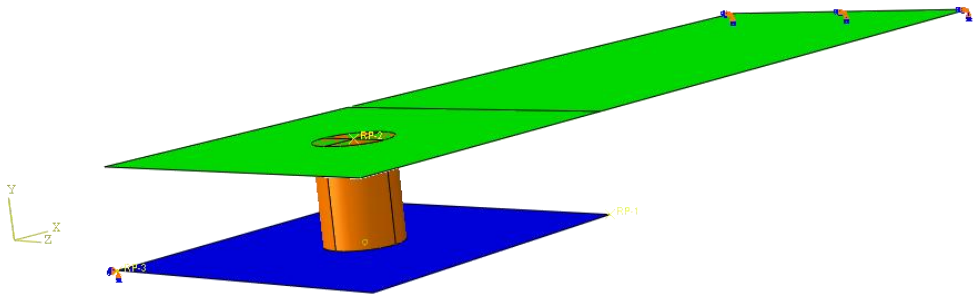

Figure I.2. Developed model to reproduce the experimental study of Mitrossilis et al. with cylinder like cell. Green: Flexible top plate. Orange: Cell. Blue: Rigid lower plate.

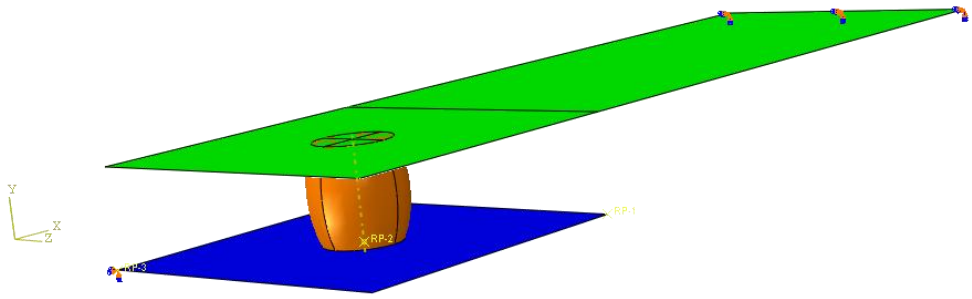

Figure I.3. Developed model to reproduce the experimental study of Mitrossilis et al. with barrel like cell. Green: Flexible top plate. Orange: Cell. Blue: Rigid lower plate.

The cell properties for the active part are set according to the model described in the Main Report, in section 2.1. Material model. The passive components follow the behaviours listed in section 2.3. Behaviour of the passive component of the cytoskeleton. With these settings and varying the elastic modulus of the top plate to achieve different values of stiffness, several cellular responses can be measured.

The boundary conditions applied to the model are:

- Right end of the flexible top plate totally fixed.
- Cell in contact with top and lower plate. The contact can be without roughness, totally attached or with enough friction to allow cell attaching but also movement.
- Lower plate totally fixed.

The stiffness of the flexible top plate comprises a range from 15 to 1800 nN/μm to address with the stiffness values employed to determine the cell exerted by the cell.

Since contact modelling is a challenging task, the cell shape was simplified to a cylinder with the contact interfaces totally attached to both plates. When the convergence was achieved for a wide variety of cantilever stiffnesses, friction coefficients were tested, aiming to a compromise value that allows cell spreading and enough attaching to the substrate. Then, cell shape was changed to an oval shape, increasing the similitude between the Mitrossilis et al. experiment and the computational model.

3.1. Model application with linear elastic behaviour of the passive component.

As first approach to the Mitrossilis et al. experiment the cell was modelled with a linear elastic behaviour of the passive component of the model. Two models were tested: Cylinder like cell and barrel like cell.

3.1.1. Cylinder like cell.

During the cell contraction, the shape changes as showed in figure I.4, where it can be observed how the cell shrinks axially and changes its shape from a cylinder to a concave form.

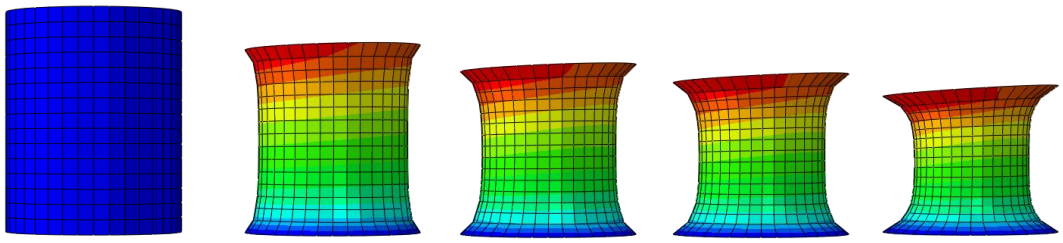

Figure I.4. Evolution of cell shape along the contraction process with a cylinder like cell.

After several calculations with a wide variety of top plate stiffnesses it can be assumed that the axial strain of the cell is higher when the substrate is less stiff. Nevertheless, applying higher stiffnesses, the axial deformation becomes smaller, increasing the transversal strain. This behaviour can be observed in the following pictures, where five representative results are showed. The stiffness of the lower plate for these cases are, in order of appearance: 15 nN/μm, 100 nN/μm, 176 nN/μm, 200 nN/μm and 750 nN/μm.

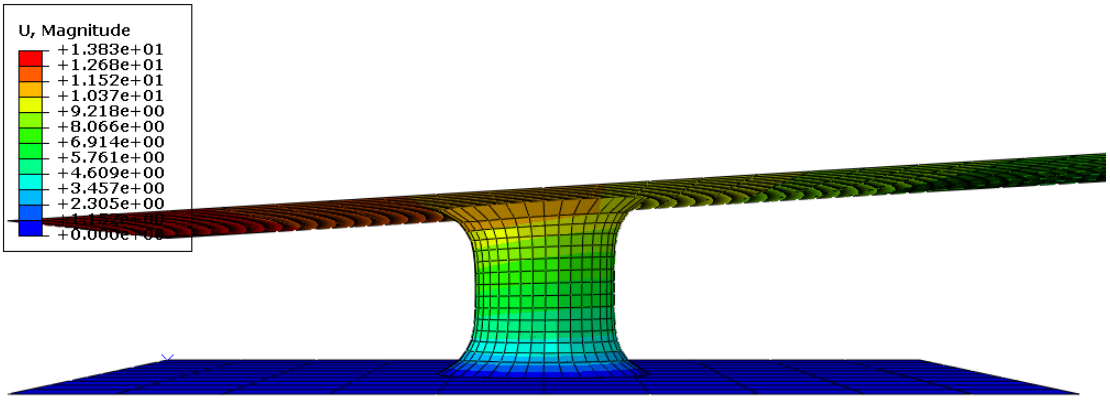

Figure I.5. Cylinder like cell displacement with linear elastic passive behaviour. Flexible top plate stiffness: 15 nN/µm.

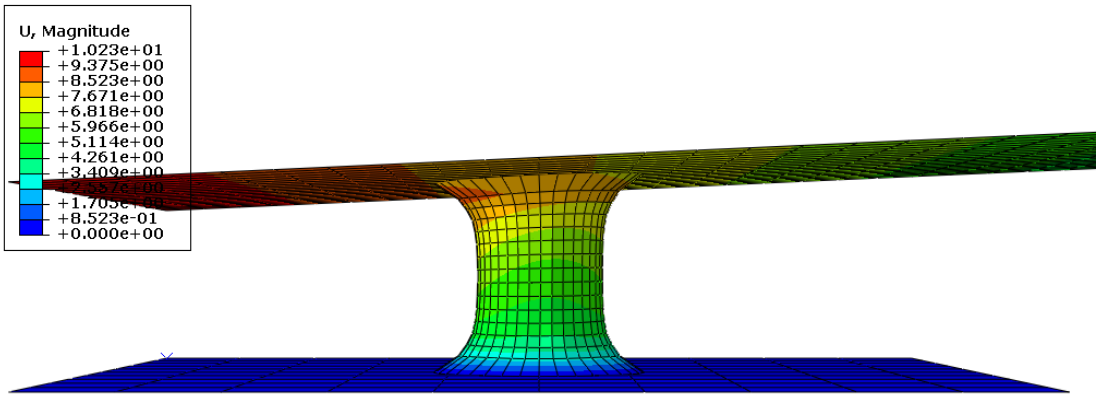

Figure I.6. Cylinder like cell displacement with linear elastic passive behaviour. Flexible top plate stiffness: 100 nN/µm.

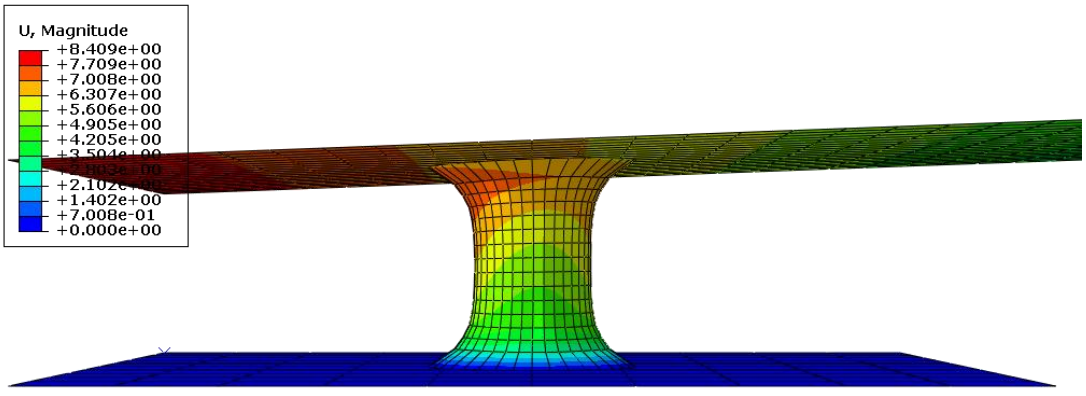

Figure I.7. Cylinder like cell displacement with linear elastic passive behaviour. Flexible top plate stiffness: 176 nN/µm.

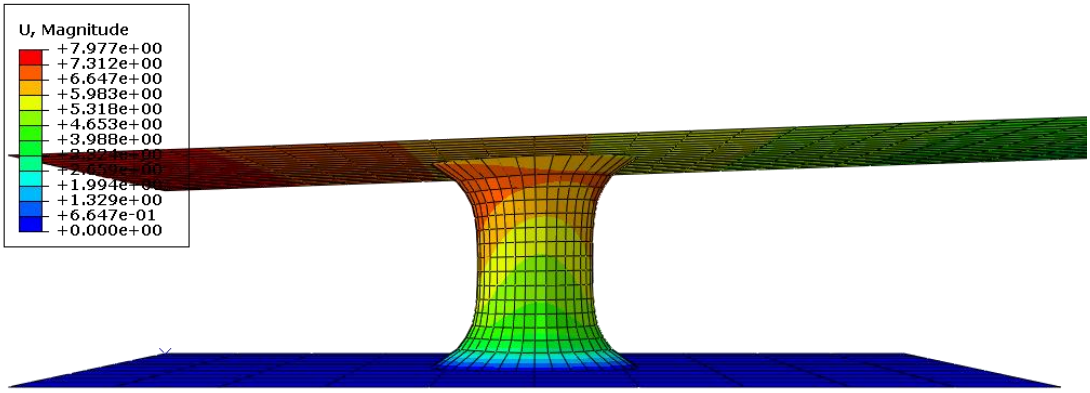

Figure I.8. Cylinder like cell displacement with linear elastic passive behaviour. Flexible top plate stiffness: 200 nN/µm.

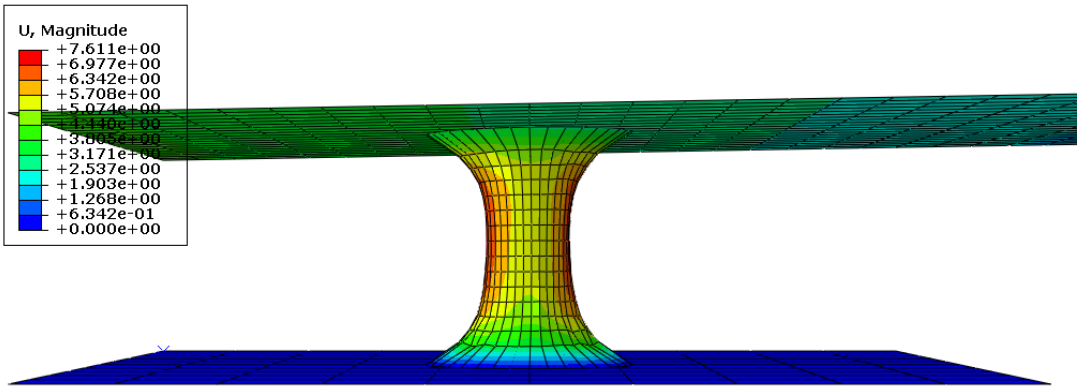

Figure I.9. Cylinder like cell displacement with linear elastic passive behaviour. Flexible top plate stiffness: 750 nN/µm.

Additionally, the cell without the top and the lower plate is exposed to clarify the explanation given above. It can be seen how the axial displacement becomes smaller as the stiffness of the flexible top plate increases, in contrast to the transversal displacement.

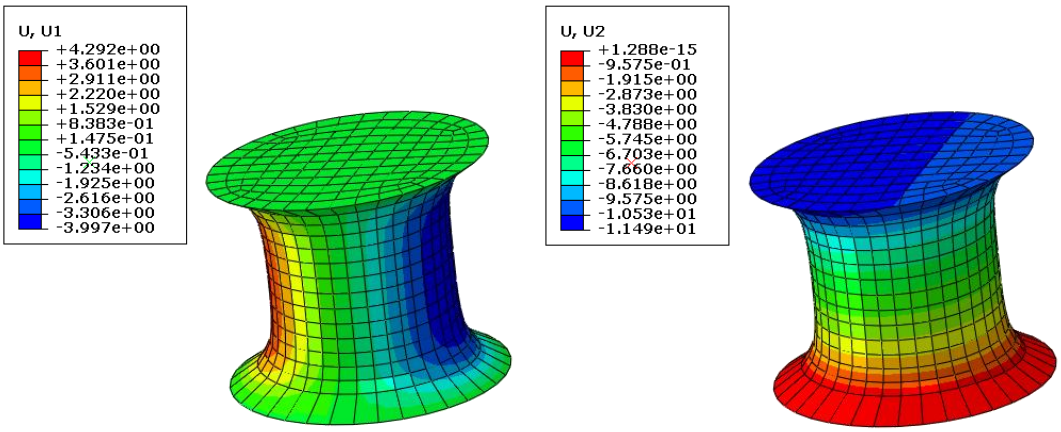

Figure I.10. Transversal (left) and axial (right) cell displacement with a flexible top plate stiffness of 15 nN/µm. Maximum transversal displacement: 4.292 µm. Maximum axial displacement: 11.490 µm.

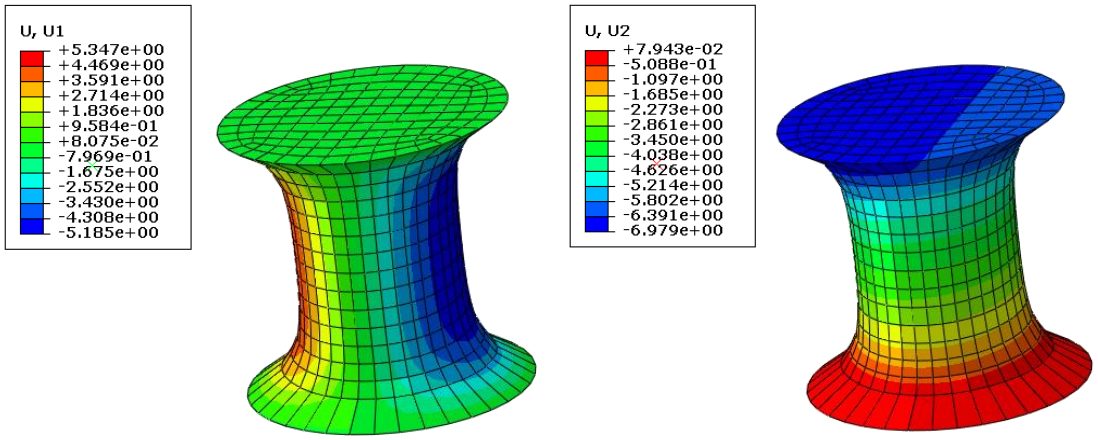

Figure I.11. Transversal (left) and axial (right) cell displacement with a flexible top plate stiffness of 176 nN/µm. Maximum transversal displacement: 5.347 µm. Maximum axial displacement: 6.979 µm.

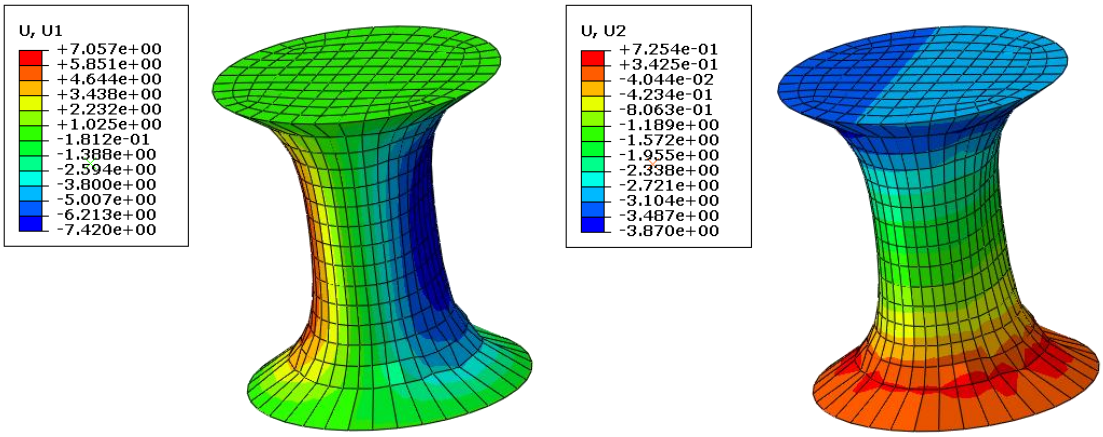

Figure I.12. Transversal (left) and axial (right) cell displacement with a flexible top plate stiffness of 750 nN/µm. Maximum transversal displacement: 7.420 µm. Maximum axial displacement: 3.870 µm.

As expected, the axial displacement of the cell decreases as the stiffness of the flexible top plate increases. However, it can be observed to higher stiffnesses that the axial displacement decreases to such degree that it is smaller than the transversal displacement. This behaviour can be explained in a way that the cell feels itself stiffness and react in consequence to its own solicitations.

To clarify this explanation, the figure I.13 is given, where it is shown how the axial displacement (blue) becomes smaller until it reach a maximum. On the other hand, the transversal contraction (red) continues increasing.

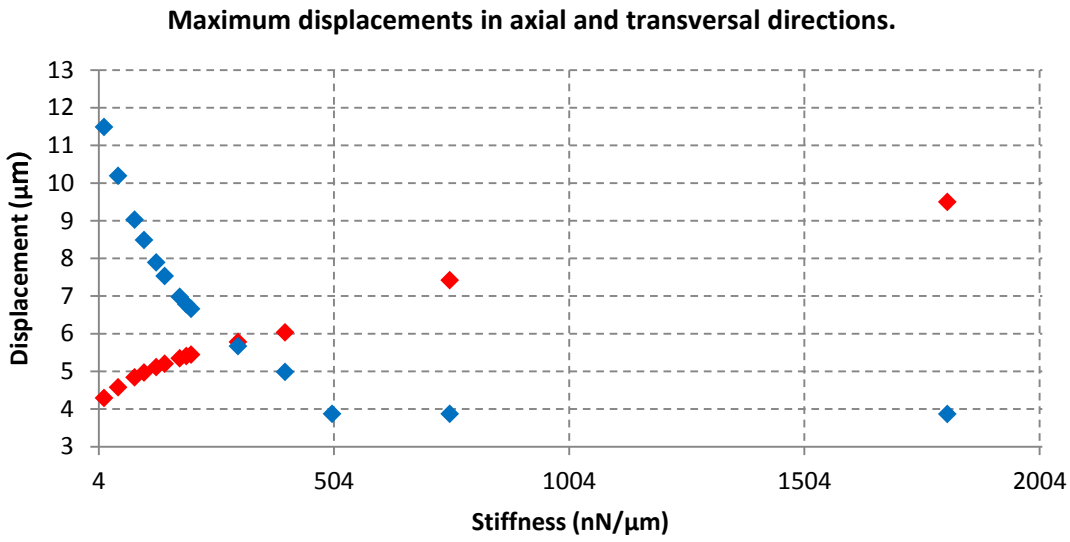

Figure I.13. Maximum displacements obtained in the cell. Passive component characterized as linear elastic. Cylinder like cell. Blue: Axial displacement. Red: Transversal displacement.

Finally, after the development of the calculations with several stiffnesses of the flexible top plate with the cylinder like cell, the forces exerted by the cell are shown in figure I.14.

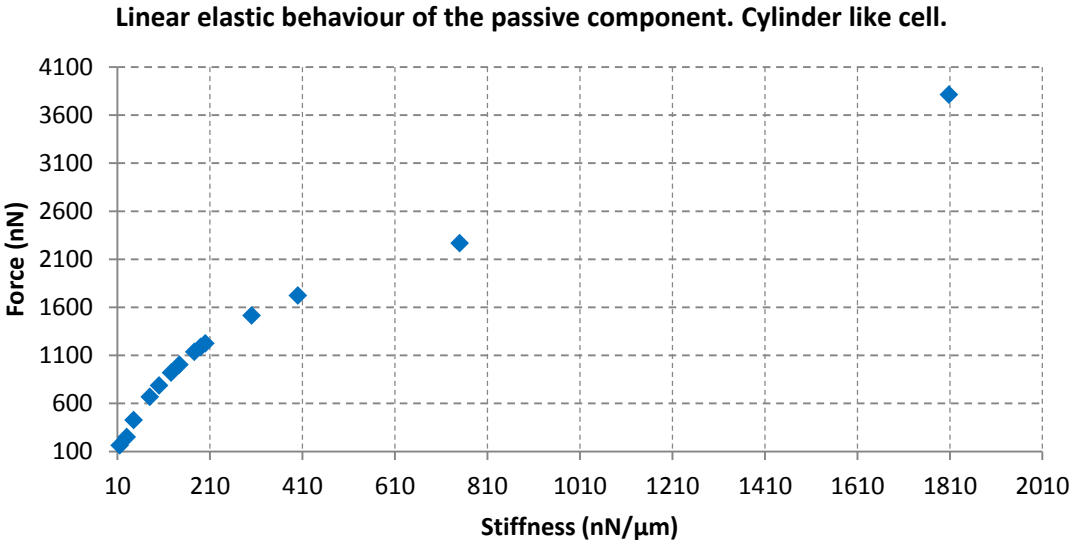

Figure I.14. Force obtained for different stiffness values. Passive component characterized as linear elastic. Cylinder like cell.

In spite of the appropriate cell behaviour observed when it changes its shape, a plateau force is not achieved. Although it can be observed a change in the trend of the force exerted by the cell when it reaches 200 nN/µm, it is not enough to stabilize the force to a same value.

Therefore, an improvement in the model is needed. The first step is changing to another suitable cell shape.

3.1.2. Barrel like cell.

In order to make a better match with the Mitrossilis et al. experiment, the cell shape is changed to a barrel like cell. The cell shape during the contraction follows the process that can be seen in figure I.15. The cell shrinks axially and changes its shape. However, the concave final shape cannot be observed as clearly as in the previous section.

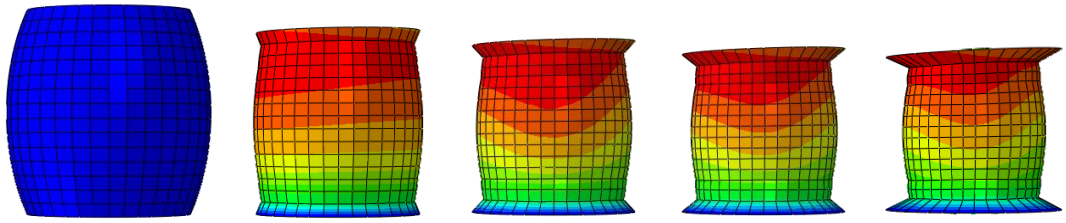

Figure I.15. Evolution of cell shape along the contraction process with a barrel like cell.

On the other hand, the characteristic results of this model, taking into account different stiffnesses, are shown below.

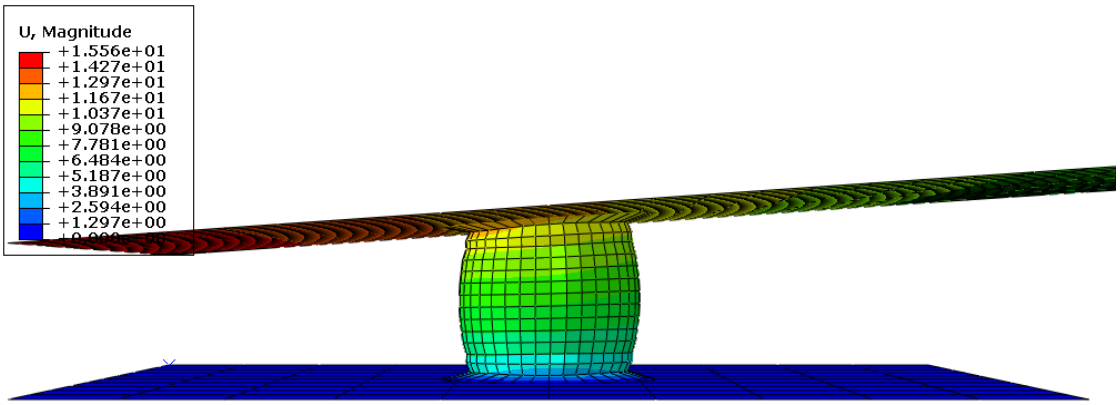

Figure I.16. Barrel like cell displacement with linear elastic passive behaviour. Flexible top plate stiffness: 15 nN/µm.

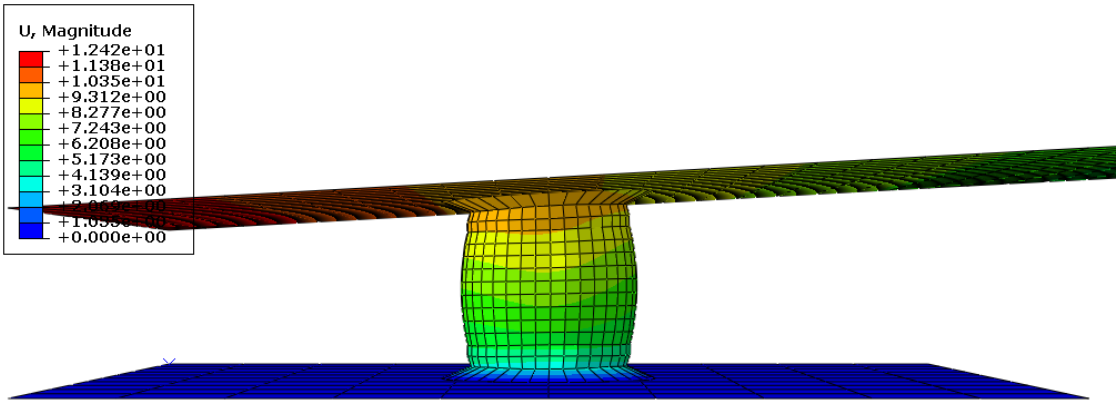

Figure I.17. Barrel like cell displacement with linear elastic passive behaviour. Flexible top plate stiffness: 100 nN/µm.

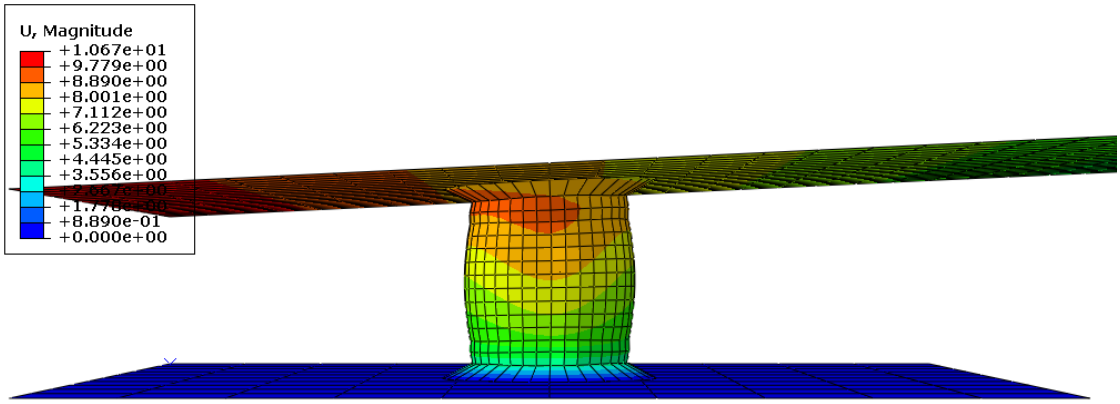

Figure I.18. Barrel like cell displacement with linear elastic passive behaviour. Flexible top plate stiffness: 176 nN/µm.

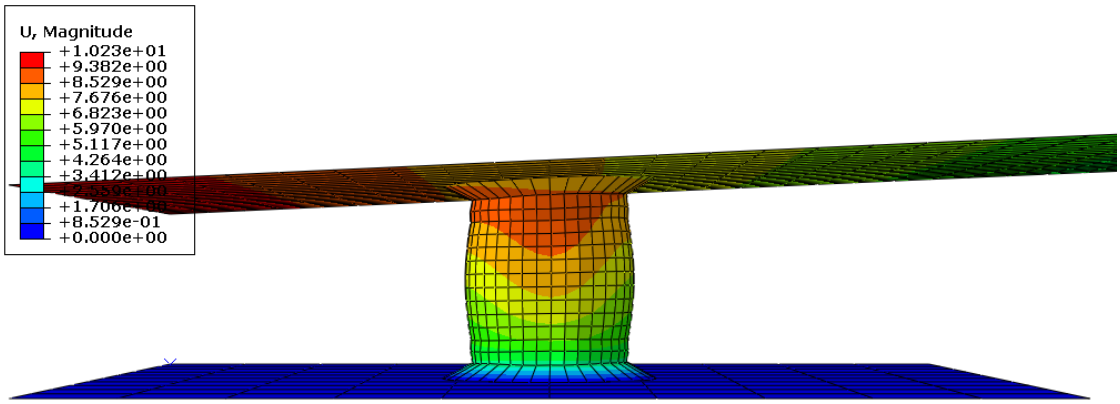

Figure I.19. Barrel like cell displacement with linear elastic passive behaviour. Flexible top plate stiffness: 200 nN/µm.

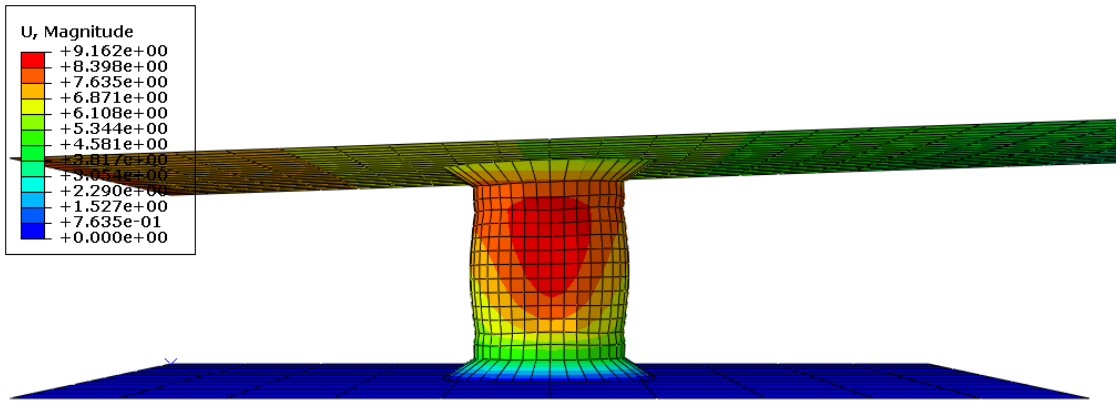

Figure I.20. Barrel like cell displacement with linear elastic passive behaviour. Flexible top plate stiffness: 400 nN/µm.

In the same way as the previous section, the axial displacement decreases as the stiffness of the flexible top plate increases. Moreover, it is observed that to higher stiffnesses the axial displacement decreases to such degree that it is smaller than the transversal displacement. The summary of these results can be seen in the figure I.21.

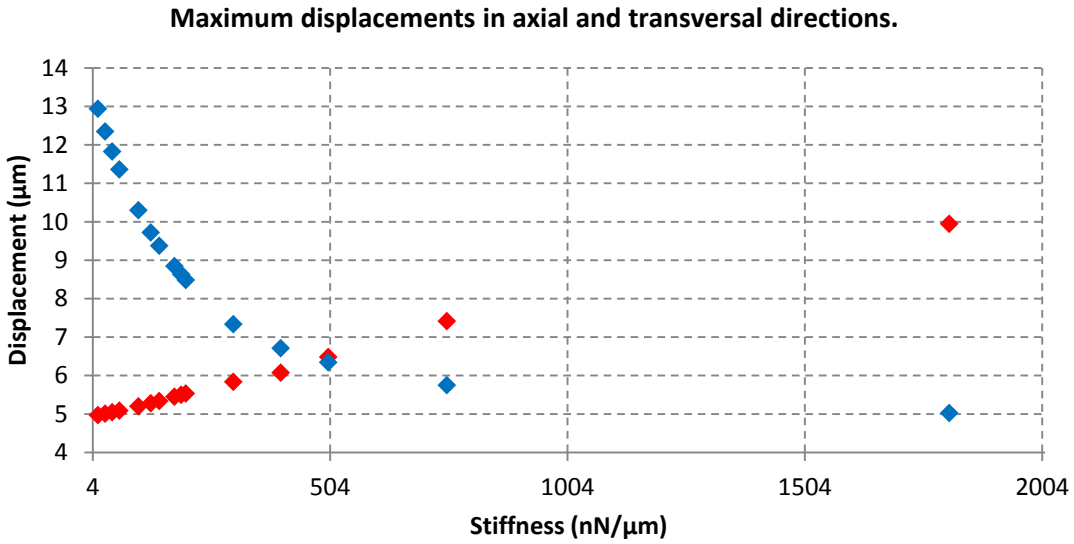

Figure I.21. Maximum displacements obtained in the cell. Passive component characterized as linear elastic. Barrel like cell. Blue: Axial displacement. Red: Transversal displacement.

The main difference with the previous case is that the axial displacement does not reach a maximum value for the studied values and also, the behaviour of the transversal displacement is close to be linear.

Eventually, using the same values for the flexible top plate and changing the cell shape, the forces exerted by the cell are the showed below.

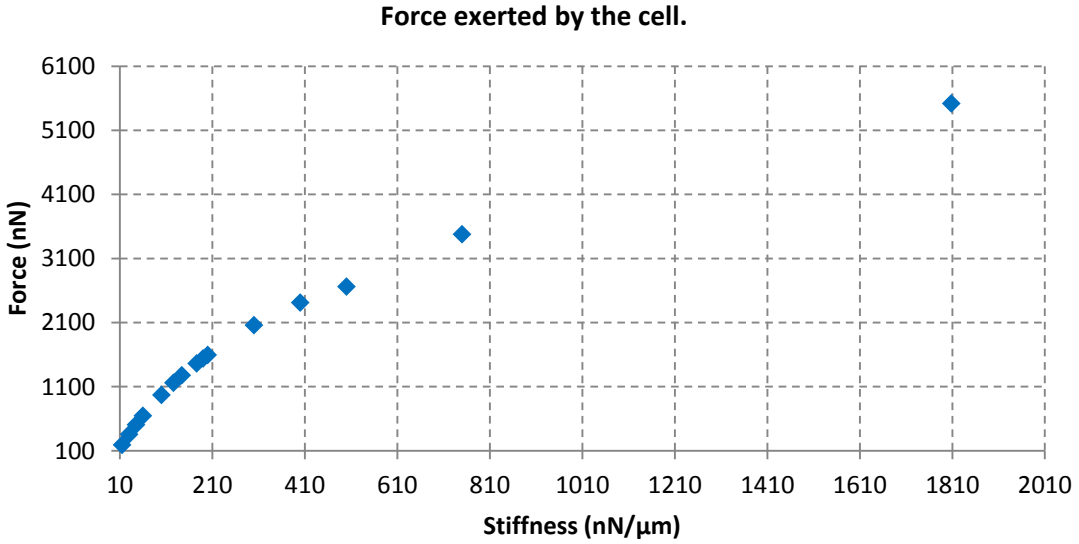

Figure I.22. Force obtained for different stiffness values. Passive component characterized as linear elastic. Barrel like cell. Each point corresponds to each result of the model.

Even though the cell shape matches better with the actual experiment of Mitrossilis et al., the cell deformation as well as the exerted force does not agree with the expected behaviour; that is, no plateau force is achieved.

Thus, the next step is to change the behaviour of the passive side of the cell to a more complex one in order to increase the significance of the model.

3.2. Model application with poroelastic behaviour of the passive component.

Looking for a better agreement with a real cell, another passive behaviour is proposed, based on a poroelastic model explained in the Main Report. Moreover, the contact behaviour is changed from a totally attached contact to a contact with friction to allow the cell certain movement along the surface. In this way, the cell is free to spread between the plates as in the actual experiment.

During the contraction process, the cell shape varies as seen in figure I.23. The main difference with the previous models is that, allowing certain cell movement, the contour behaves in a different way, without sharp edges on the contact at the end of the contraction process. In addition, the cell preserves its shape and volume more than in the previous cases with the linear elastic passive behaviour.

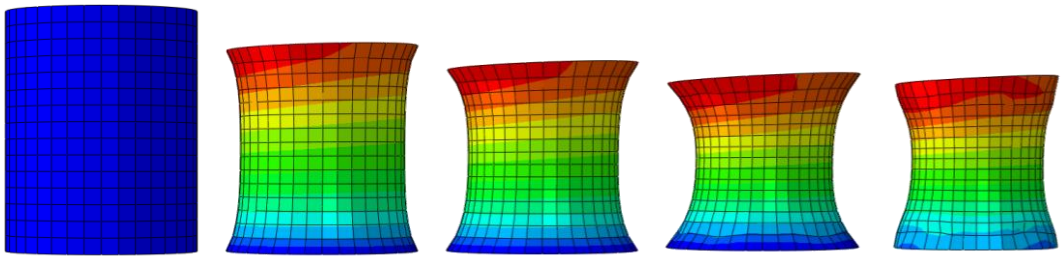

Figure I.23. Evolution of cell shape along the contraction process with a cylinder like cell and poroelastic behaviour.

Therefore, there were tested the same previous cases changing the behaviour of the passive side of the cell and the behaviour of the contact. The displacements obtained for the most representative calculations after the application of several stiffnesses in the cantilever beam are showed below.

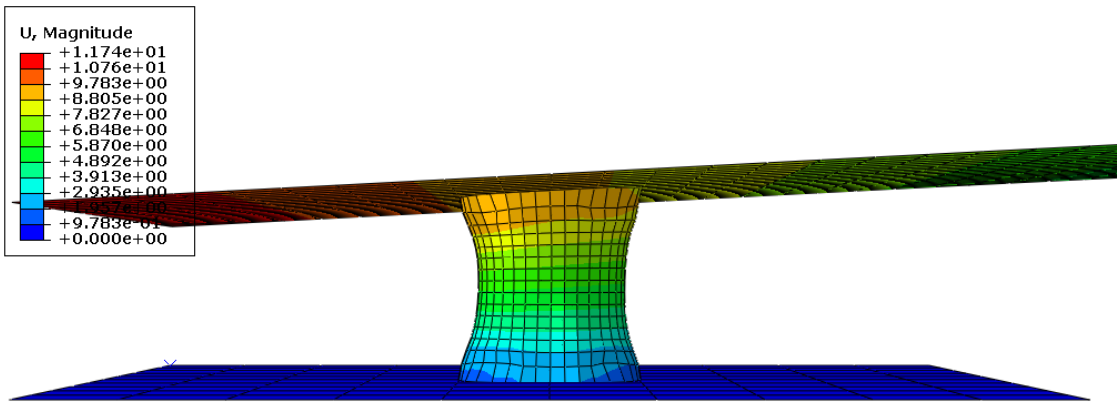

Figure I.24. Cell displacement with poroelastic passive behaviour. Flexible top plate stiffness: 15 nN/µm.

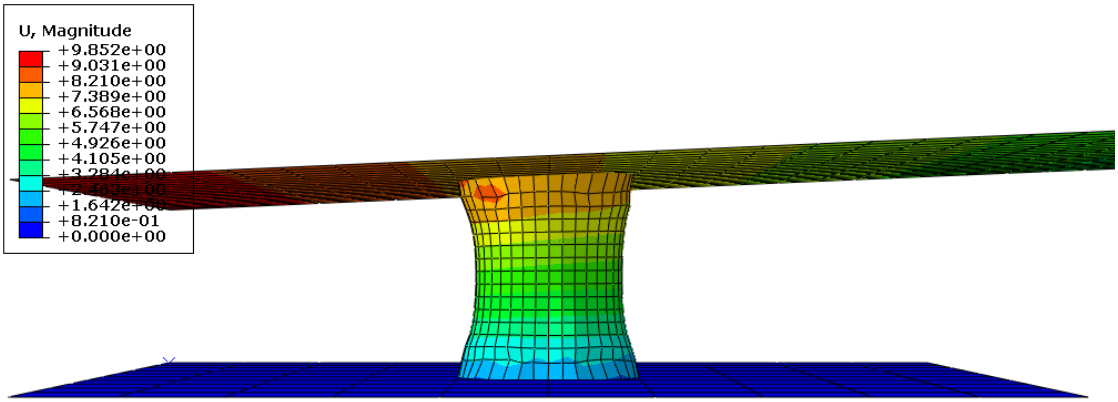

Figure I.25. Cell displacement with poroelastic passive behaviour. Flexible top plate stiffness: 100 nN/μm.

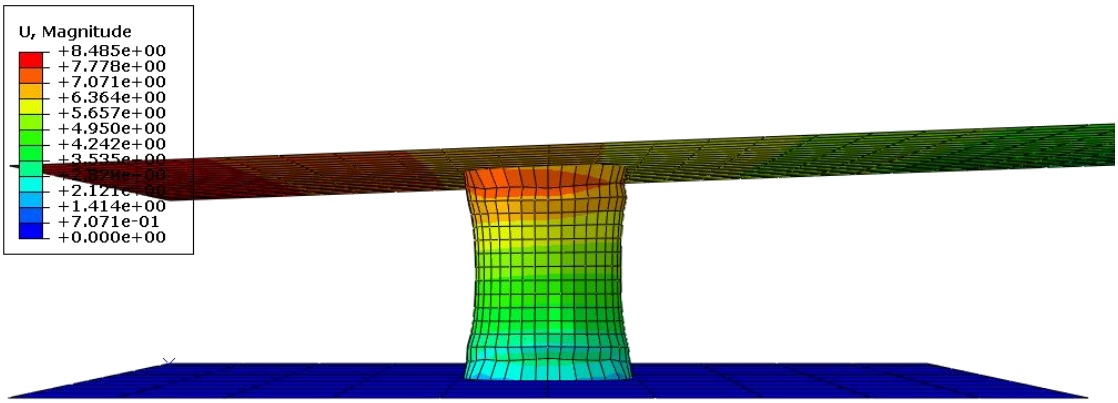

Figure I.26. Cell displacement with poroelastic passive behaviour. Flexible top plate stiffness: 176 nN/μm.

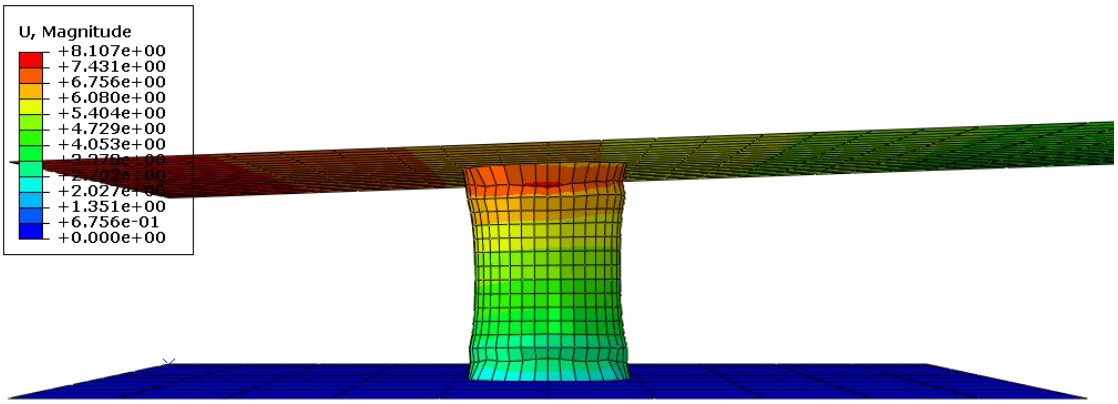

Figure I.27. Cell displacement with poroelastic passive behaviour. Flexible top plate stiffness: 200 nN/μm.

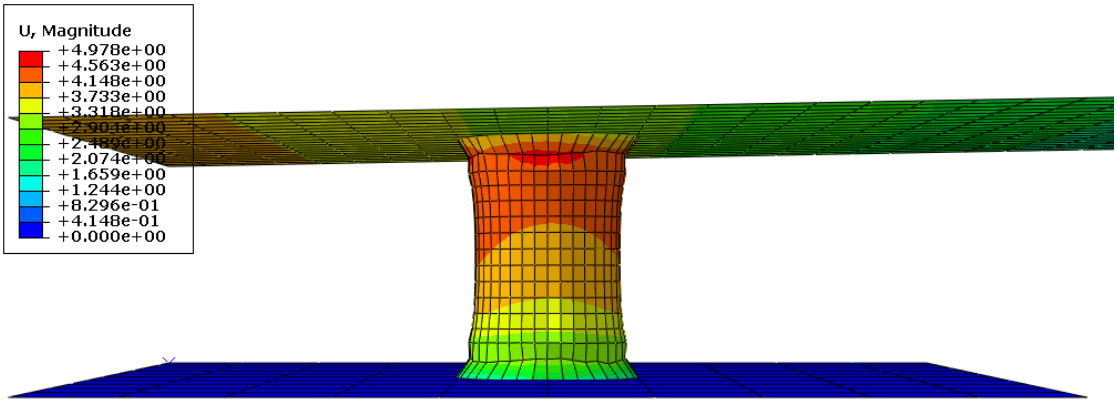

Figure I.28. Cell displacement with poroelastic passive behaviour. Flexible top plate stiffness: 750 nN/µm.

Making a further study of the cell displacements, the main results are shown in the figures I.29, I.30 and I.31.

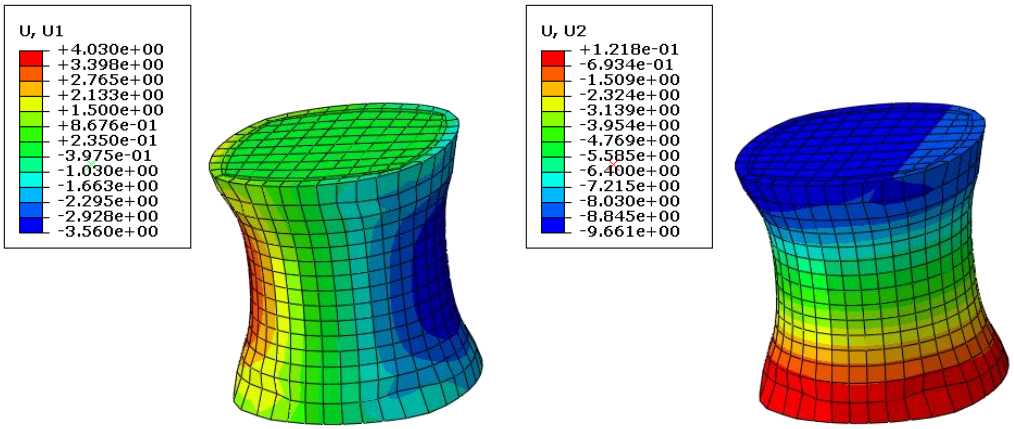

Figure I.29. Transversal (left) and axial (right) cell displacement with a flexible top plate stiffness of 15 nN/µm. Maximum transversal displacement: 4.030 µm. Maximum axial displacement: 9.661µm.

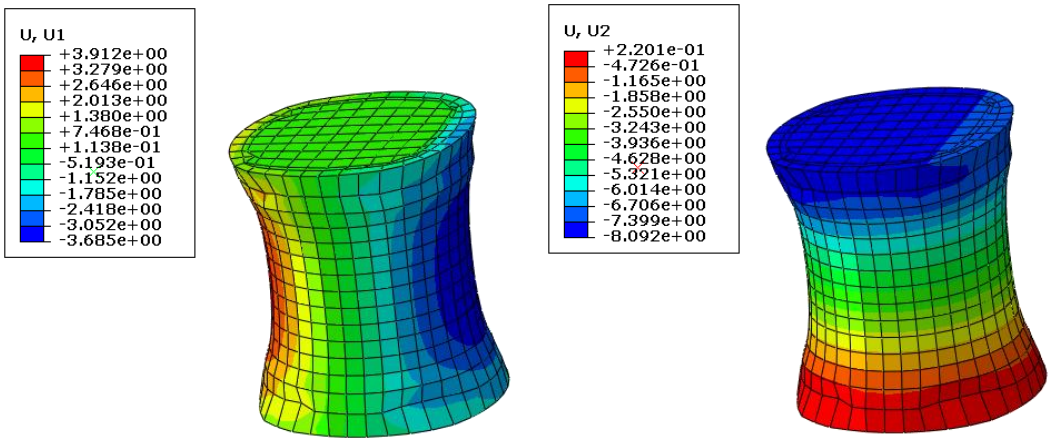

Figure I.30. Transversal (left) and axial (right) cell displacement with a flexible top plate stiffness of 100 nN/µm. Maximum transversal displacement: 3.912 µm. Maximum axial displacement: 8.092 µm.

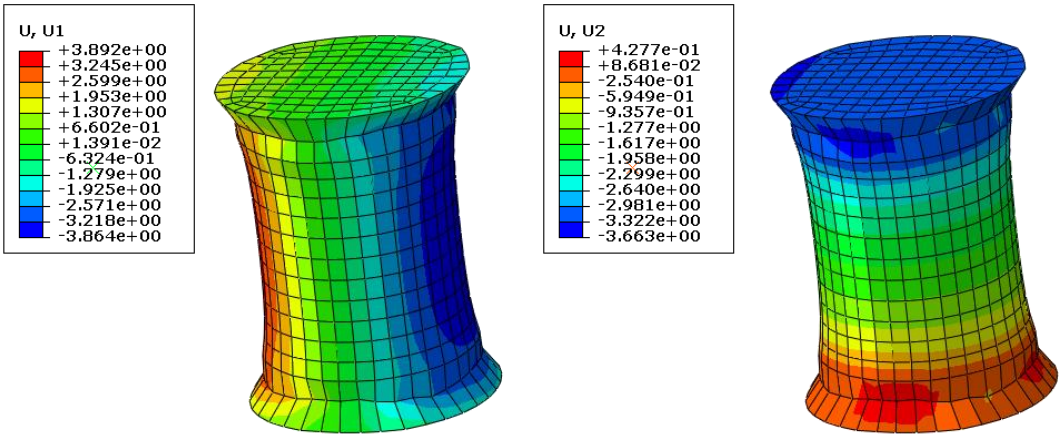

Figure I.31. Transversal (left) and axial (right) cell displacement with a flexible top plate stiffness of 750 nN/µm. Maximum transversal displacement: 3.892 µm. Maximum axial displacement: 3.663 µm.

Similarly to the previous cases, the axial displacement of the cell decreases as the stiffness of the flexible top plate increases. Nevertheless, the transversal displacement tends to stabilize after it reaches the maximum, possibly due to the poroelastic behaviour of the passive side. Although the axial displacement does not follow the same trend, it must be taken into account not only the stiffness of the top plate but also the shape of the cell on the plates that makes the cell has more material in one direction than another.

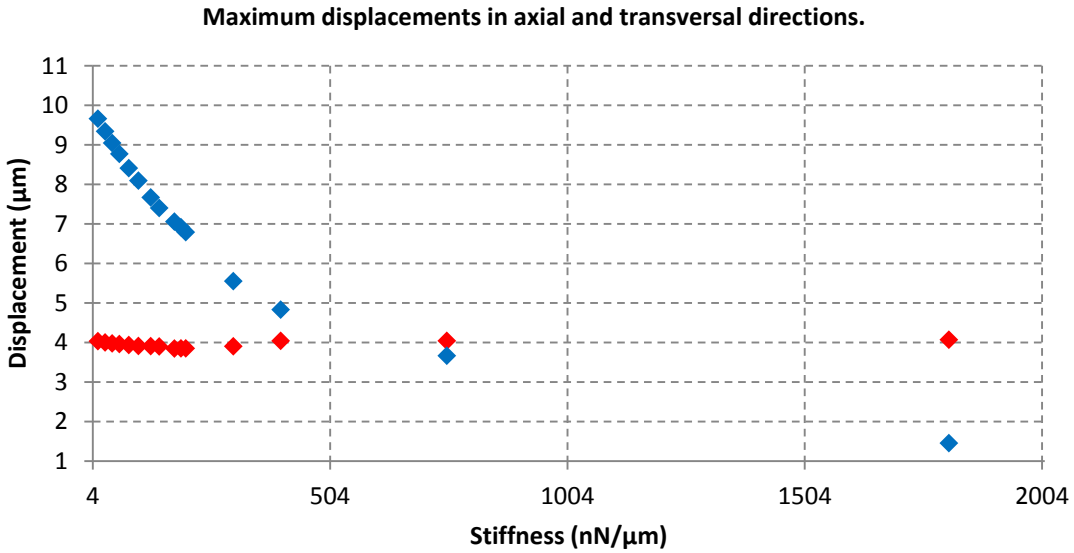

Figure I.32. Maximum displacements obtained in the cell. Passive component characterized as poroelastic. Cylinder like cell. Blue: Axial displacement. Red: Transversal displacement.

Finally, after the calculation of several cell models with different top plate stiffnesses, it can be obtained the results showed in figure I.33, where it can be observed the trend of the cell force as the stiffness increases.

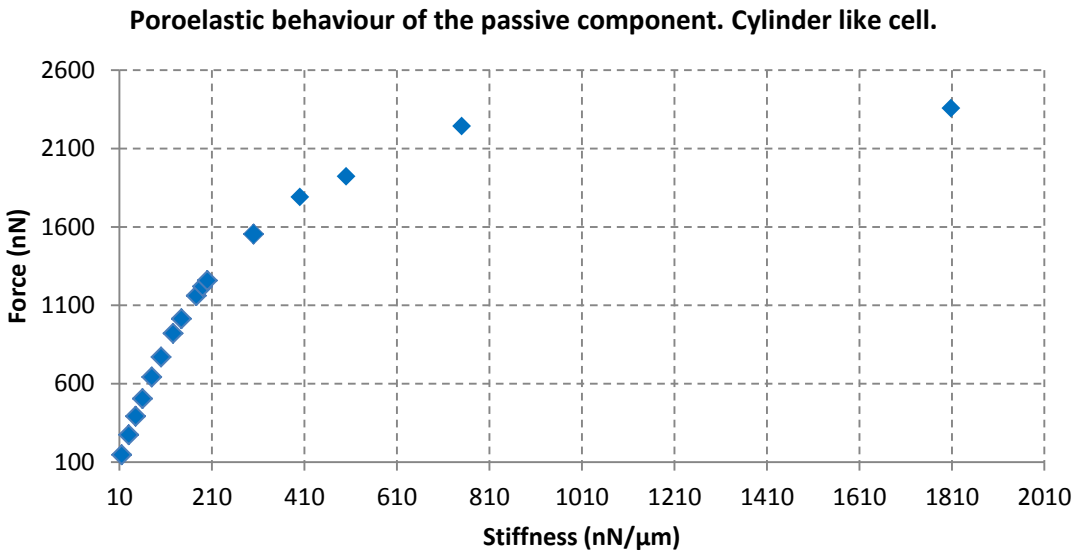

Figure I.33. Force obtained for different stiffness values. Passive component characterized as poroelastic. Cylinder like cell. Each point corresponds to each result of the model.

The main difference with the models above, in which a linear elastic behaviour of the passive side is employed, is that the cell reaches a plateau force established between 2200 nN and 2400 nN once the stiffness of the flexible top plate is set to 750 nN/µm.

Nevertheless, although the force exerted by the cell behaves properly, reaching a maximum force after a specific stiffness, the shape development does not agree with the observed in the experiment, in which the cell shrinks axially and spreads transversally. A feasible explanation of this behaviour is given in the conclusion section of the Main Report.

4. Model application to real cell geometry.

On the other hand, taking advantage of the relationship between this University and the CIMA, there was studied a real cell model. The cellular model is based on a breast cancer cell line MDA-MB-231 cultured using microfluidic devices. The cell was imaged under confocal microscopy slice by slice over the Z axis, with 1 µm distance between them.

After the segmentation to smooth the cell boundary and to give the cytoskeleton staining, the segmented cell is transformed into a cloud of points through the sampled points obtained at the cell boundary. Then, the cell is discretized into three-dimensional volumes via tetrahedralization, which creates the elements to work with the finite element model.

Hence, the cell is characterized in the same way as the previous case, with a passive and an active side, duplicating the elements.

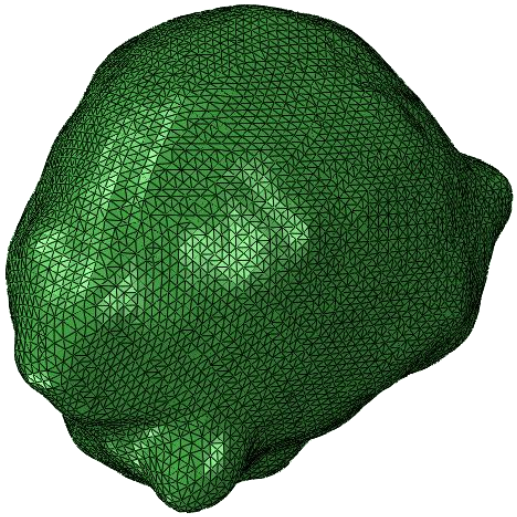

Figure I.34. Cellular model obtained in the Centro de Investigación Médica Aplicada of Navarra.

4.1. Cell embedded in a substrate.

As first approach, the cell is embedded in a cubic substrate of 194 μm side characterized both as linear elastic and hyperelastic behaviour. The values are 1 KPa and a Poisson ratio of 0.49 for the linear elastic model. Then, for the hyperelastic behaviour, the values for the characterization are obtained via uniaxial test. The parameters are given in the table I.1.

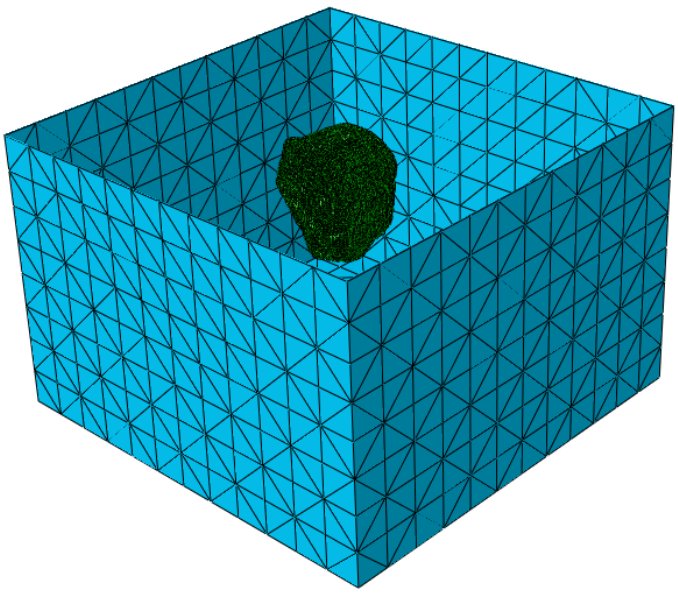

Figure I.35. Cellular model (green) inside the substrate (blue).

σ_n	λ
0.304905	9.9995e-05
0.436859	0.000145989
0.631863	0.000213977
0.913933	0.000312951
1.32549	0.000457895
1.90341	0.000668776
2.76873	0.000977522
4.01796	0.00142898
5.81187	0.00208782
8.43461	0.00305533
12.197	0.00446004
17.5809	0.00651871
25.2385	0.0095245
35.9336	0.0139029
50.3498	0.0202927
68.0394	0.0294617
86.6822	0.0428679
102.604	0.0620354
112.008	0.089475
113.088	0.128393
106.74	0.182322

Table I.1. Hyperelastic parameters, where σ_n is the nominal stress in kPa and λ is the nominal strain.

On the other hand, the cell properties are set as linear elastic with an elastic modulus of 75 KPa and near-incompressible behaviour with a Poisson ratio of 0.49. It must be taken into account that, unlike a real cell, this cell is totally attached to the substrate and, hence, it can exert force around its entire surface.

This model has 1074096 C3D4 elements divided as follows:

- 529648 elements corresponding to the substrate.
- 272223 elements corresponding to the passive side of the cell.
- 272223 elements corresponding to the active side of the cell.

Finally, the boundary conditions are applied to the substrate surface, making it totally fixed in order to allow the cell to feel the mechanical properties of its surrounding matrix.

4.1.1. Linear elastic substrate application.

After the model application to the cell geometry with the linear elastic substrate, the results are shown in the figures I.36 and I.37.

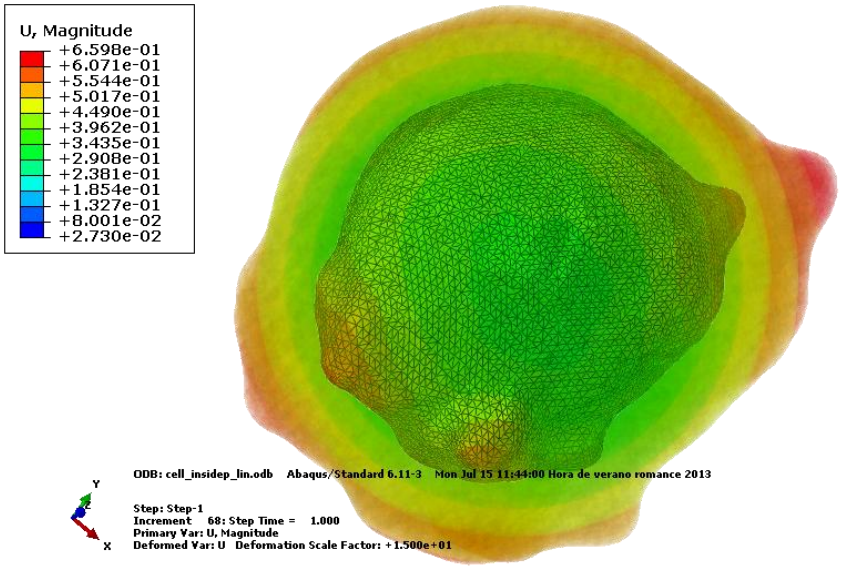

Figure I.36. Side view of the cell contraction obtained after the model application. Undeformed shape (translucent) and deformed shape (inside). Displacement displayed. It can be observed a cell contraction between 0.66 and 0.03 μm. Scale factor: 15.

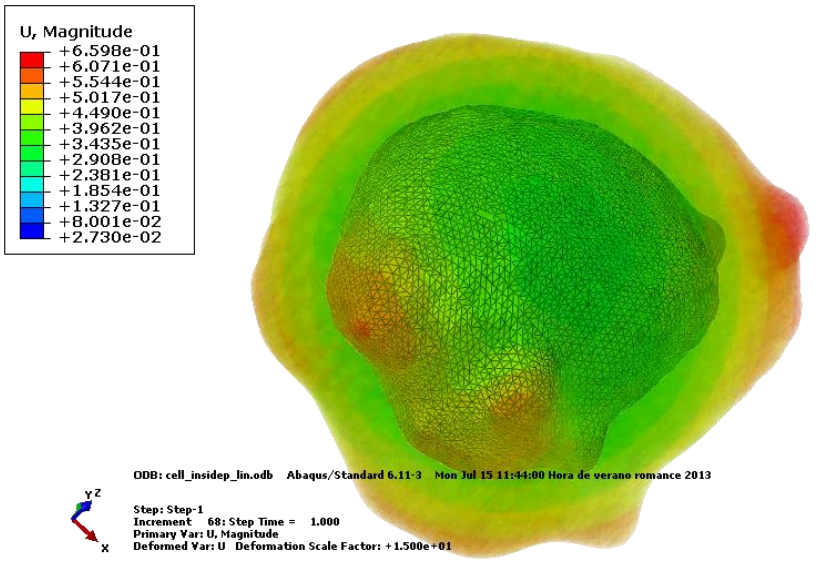

Figure I.37. Side view of the cell contraction obtained after the model application. Undeformed shape (translucent) and deformed shape (inside). Displacement displayed. It can be observed a cell contraction between 0.66 and 0.03 μm. Scale factor: 15.

As can be observed in figures I.36 and I.37, cell model involves a whole cell contraction without shape change.

4.1.2. Hyperelastic substrate application.

After the model application to the cell geometry with the hyperelastic substrate, the results are the exposed in the figures I.38 and I.39.

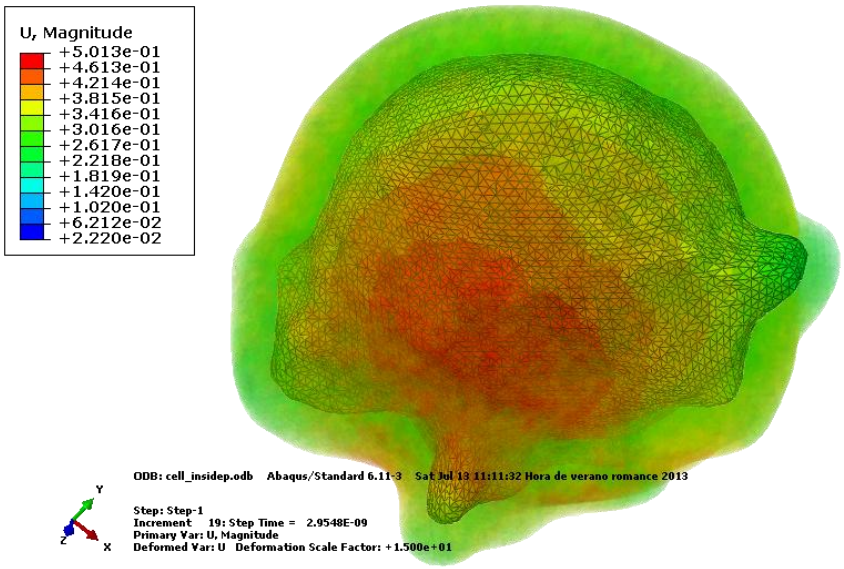

Figure I.38. Side view of the cell contraction obtained after the model application. Undeformed shape (translucent) and deformed shape (inside). Displacement displayed. It can be observed a cell contraction between 0.50 and 0.02 μm, with a protrusion accentuation. Scale factor: 15. The substrate is not displayed.

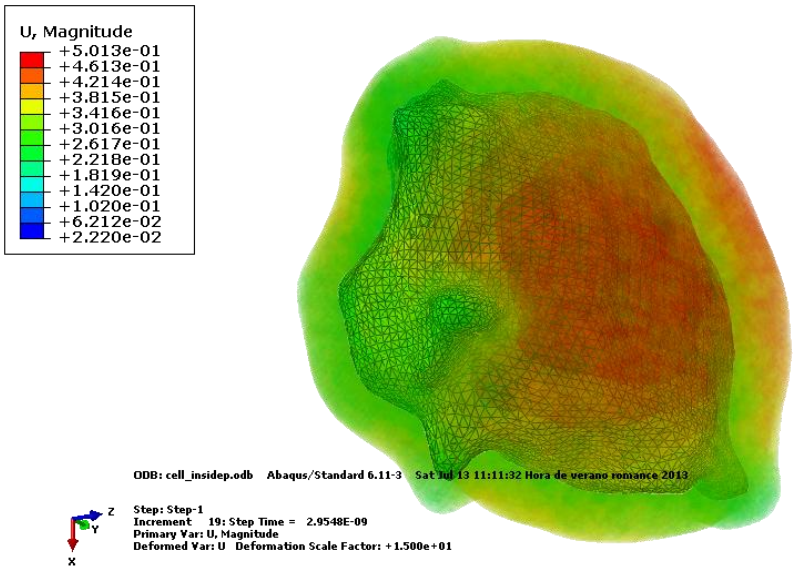

Figure I.39. Rear view of the cell contraction obtained after the model application. Undeformed shape (translucent) and deformed shape (inside). Displacement displayed. It can be observed a cell contraction between 0.50 and 0.02 μm, with a protrusion accentuation. Scale factor: 15. The substrate is not displayed.

As shown in the figures I.38 and I.39, cell model involves not only a whole cell contraction but also a protrusion accentuation, in agreement with the probing role of the lamellipodia and filopodia in mechanosensing mechanism.

4.1.3. Comparison between elastic and hyperelastic substrate.

A brief comparison of the influence in cell behaviour depending on the properties of the substrate can be observed in the figure I.40.

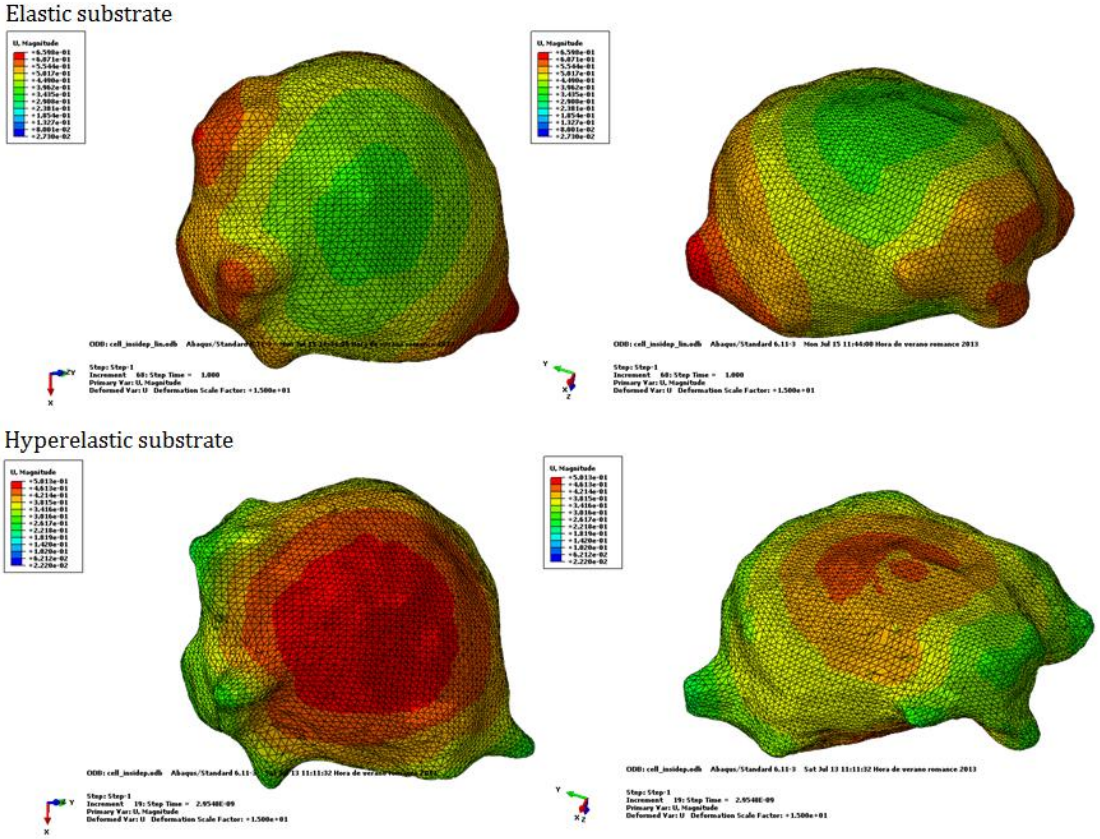

Figure I.40. Rear view of the cell contraction obtained after the model application. Undeformed shape (translucent) and deformed shape (inside). Displacement displayed. It can be observed a cell contraction between 0.50 and 0.02 μm, with a protrusion accentuation. Scale factor: 15. The substrate is not displayed.

As previously exposed, cell strain differs depending on whether the cell is in a linear elastic substrate or in a hyperelastic substrate, producing not only a whole cell contraction but also an accentuation of the protrusion in the second case.

4.2. Simulating focal adhesions.

Since the cells are not totally attached to its substrate, the case developed above must be refined. Thus, the substrate is eliminated and it is replaced by boundary conditions applied to the main protrusion that can be found on the cell surface. These boundary conditions are modelled like springs that simulate the focal adhesion that could make the cell when is embedded in its ECM. In addition, applying several stiffnesses to the springs, different kinds of the substrates can be modelled.

In this way, six adhesions around the cell surface are created, employing springs on each nodal surface of the protrusions. The spring stiffnesses range from 1 nN/μm to 2500 nN/μm aiming to simulate different substrates. The position of these adhesions is shown below:

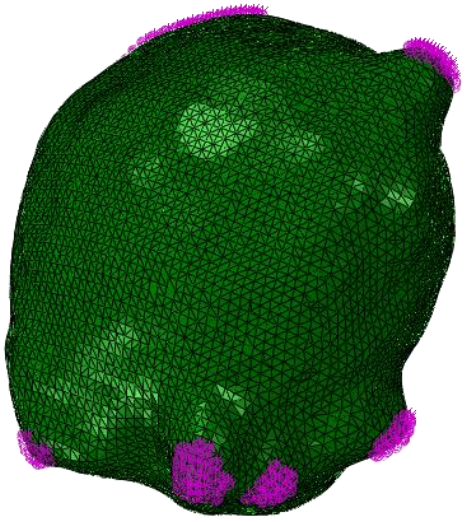

Figure I.41. Cell (green) with focal adhesions placed on the protrusions (purple).

Taking into account this kind of boundary conditions, the model is composed with a total of 545642 elements divided as follows:

- 272224 C3D4 elements corresponding to the passive side of the cell.
- 272224 C3D4 elements corresponding to the active side of the cell.
- 1194 spring elements corresponding to the focal adhesions.

4.2.1. Cell without nucleus.

Once the boundary conditions are set, the cell is modelled, as seen previously, with a linear elastic passive side with an elastic modulus of 1 kPa and a Poisson ratio of 0.45. In the same way, the active side is characterized as linear elastic with an elastic modulus of 10 kPa and a Poisson ratio of 0.45.

Following, there are exposed the principal results of the cell model, where can be observed different displacements and stresses depending on the stiffness of the focal adhesion. As expected, the minimum cell displacement occurs in the focal adhesions where it is attached whereas the cell body shrinks while it exerts force. Moreover, the stress distribution is uniform throughout the cell body, increasing in the cell adhesions.

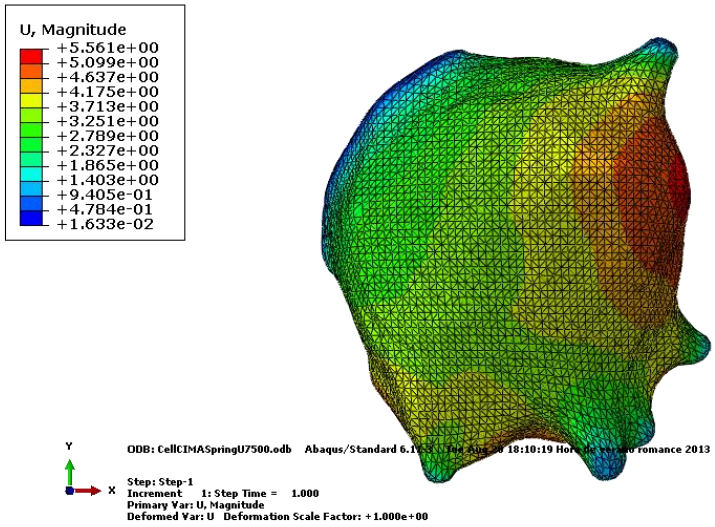

Figure I.42. Displacements obtained with 7.5 nN/µm of focal adhesion stiffness.

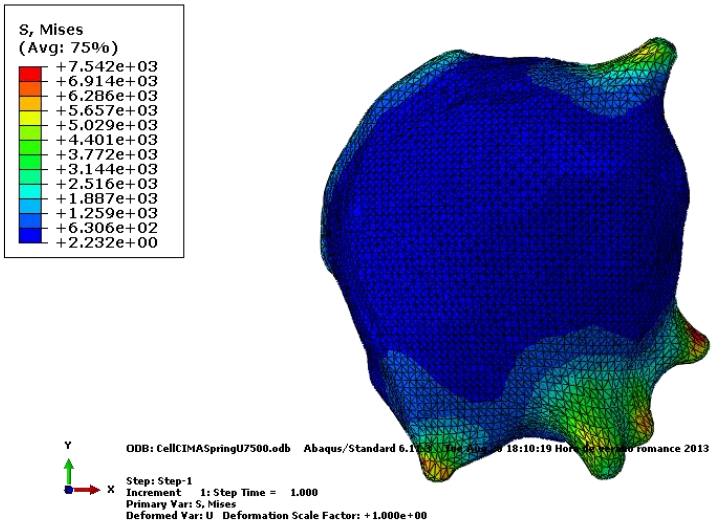

Figure I.43. Stresses obtained with 7.5 nN/µm of focal adhesion stiffness.

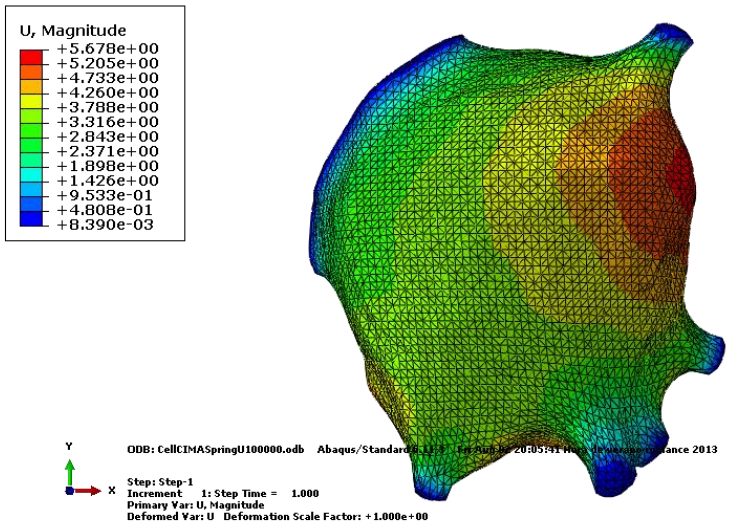

Figure I.44. Displacements obtained with 100 nN/µm of focal adhesion stiffness.

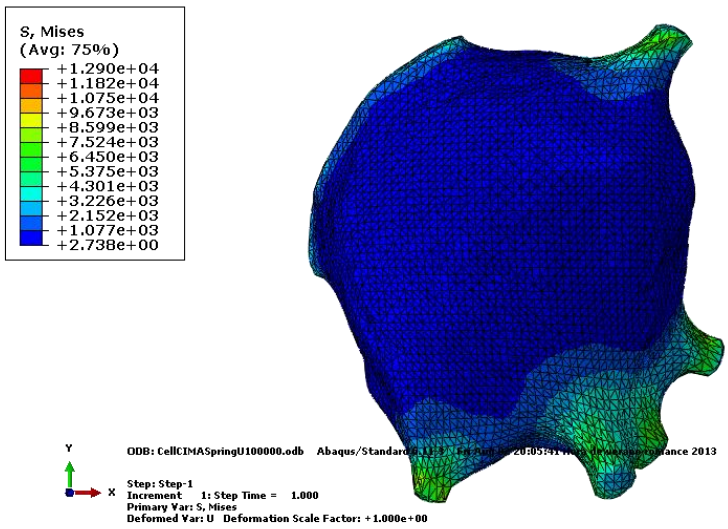

Figure I.45. Stresses obtained with 100 nN/µm of focal adhesion stiffness.

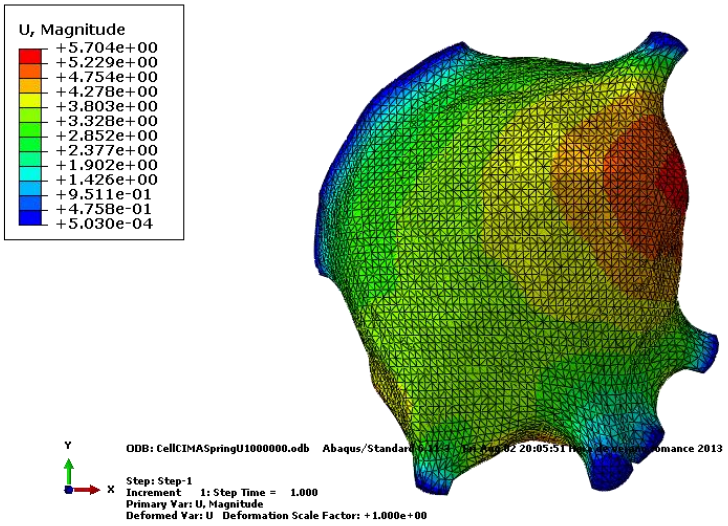

Figure I.46. Displacements obtained with 1000 nN/µm of focal adhesion stiffness.

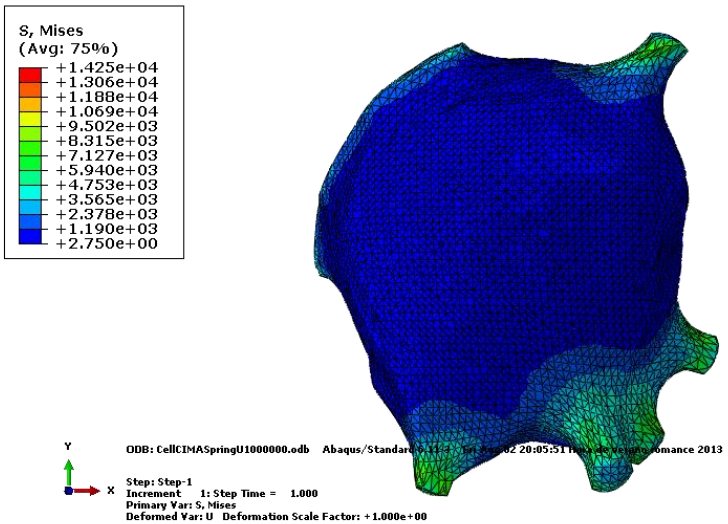

Figure I.47. Stresses obtained with 1000 nN/µm of focal adhesion stiffness.

After the analysis of the whole cell and focal adhesions displacements, the results of figure I.48 are obtained. The cell displacement initially follows a linear behaviour until the focal adhesions reach 50 nN/µm. In this point, a change in the trend occurred and the displacement reaches a maximum value of 5.7 µm for the following focal adhesion stiffnesses. Furthermore, the displacement of the focal adhesions follows an exponential behaviour, reaching the minimum to stiffer substrates.

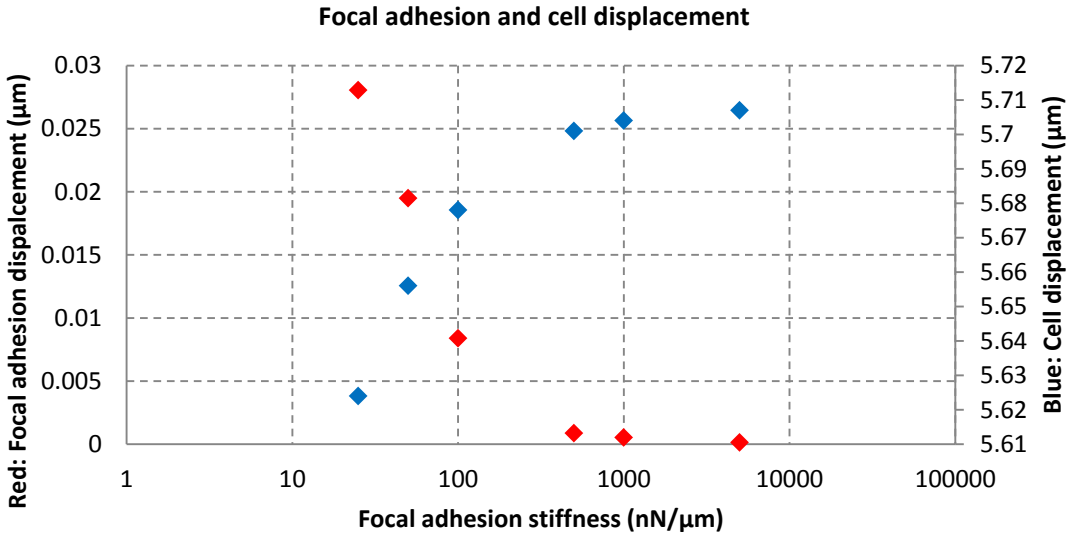

Figure I.48. Focal adhesion displacement (red) and cell displacement (blue) depending on the stiffness of the substrate.

Since Abaqus® does not allow obtaining the reaction force in this kind of boundary conditions and considering that the stress is in relationship with the force exerted by the cell, by mean of the maximum stress generated, a similar response than in the section above can be obtained, where the reaction force at the end of the flexible plate was measured.

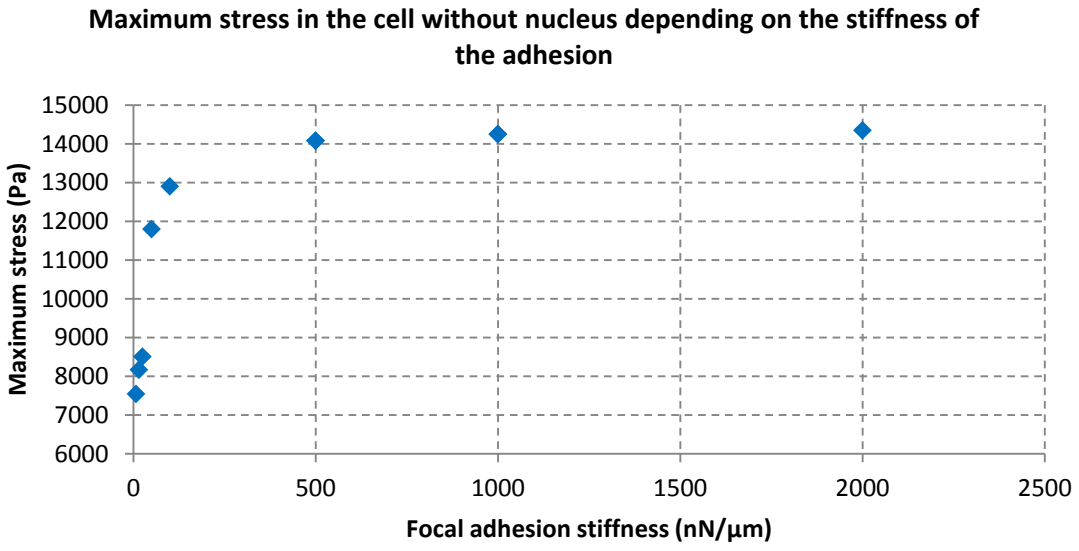

Figure I.49. Maximum stress obtained within the cell without nucleus depending on the stiffness of the simulated adhesions.

The figure I.49 shows that a plateau stress at 14.4 kPa is reached for a stiffness value of 500 nN/µm, where the cell cannot exert more force even though the substrate is stiffer.

4.2.2. Cell with nucleus.

The nucleus influence is studied in this model by mean of an element set chosen with an algorithm that selects a group of elements that is within a sphere of a given radius. In this way, even though there is no nucleus in the model, it can be created using Matlab®.

Nevertheless, since the cell model has no nucleus defined inside and the mesh is made to fulfil the requirements of the boundaries, the inner elements can be coarse, obtaining shapes with several edges. Therefore, it is considered that this approximation is enough to study the influence of the nucleus on the cell outer layers but not between the cytoskeleton and the nucleus due to the low definition of the boundary.

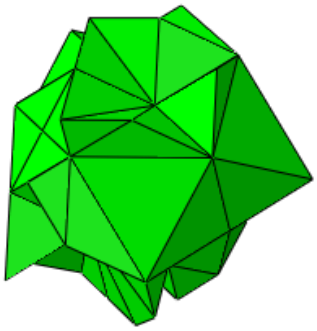

Figure I.50. Element set inside the cell characterized as cell nucleus.

To study its influence, the nucleus is modelled as a linear elastic solid 10 and 100 times stiffer than the surrounding cytoskeleton, namely 10 kPa and 100 kPa; and without contraction properties.

a) Cell nucleus with an elastic modulus of 10 kPa.

Applying an elastic modulus of 10 kPa to the cell nucleus, three main results can be seen below with three cutting planes that allow seeing inside the cell to observe the nucleus behaviour.

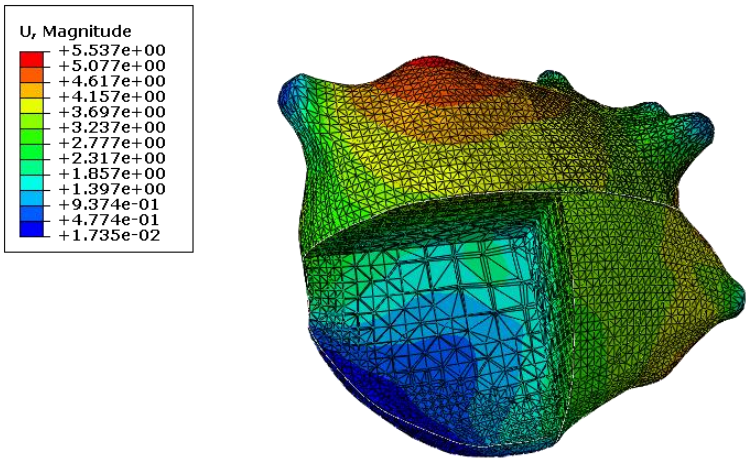

Figure I.51. Displacements obtained with 7.5 nN/µm of focal adhesion stiffness.

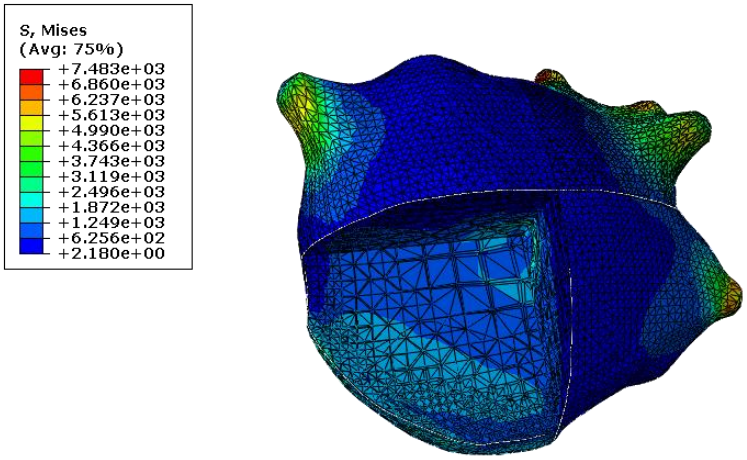

Figure I.52. Stresses obtained with 7.5 nN/µm of focal adhesion stiffness.

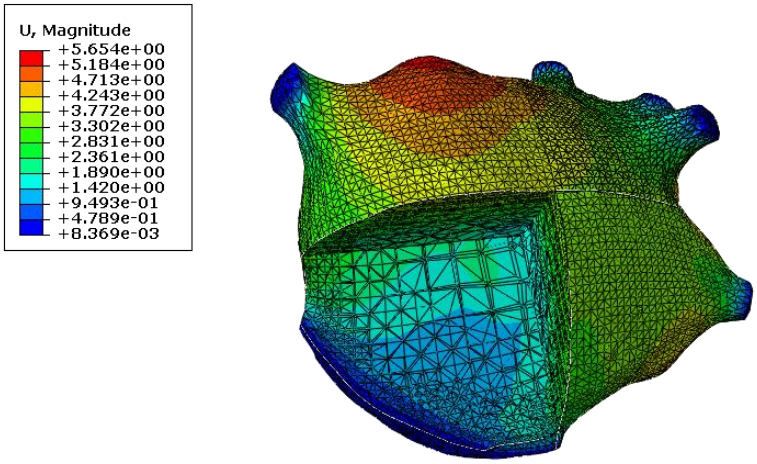

Figure I.53. Displacements obtained with 100 nN/µm of focal adhesion stiffness.

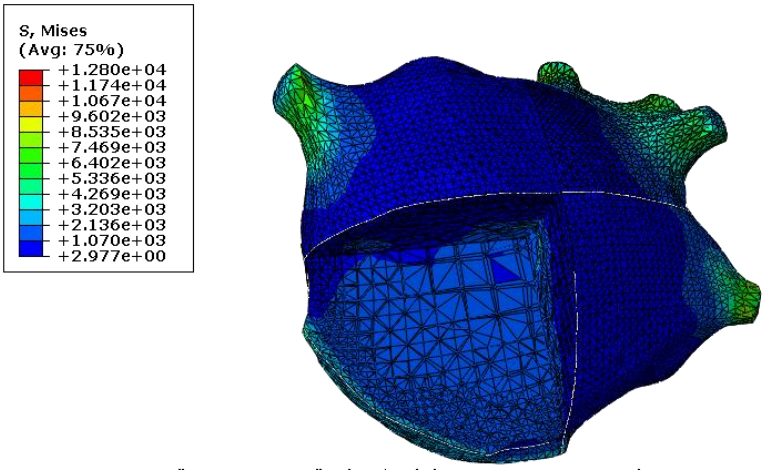

Figure I.54. Stresses obtained with 100 nN/µm of focal adhesion stiffness.

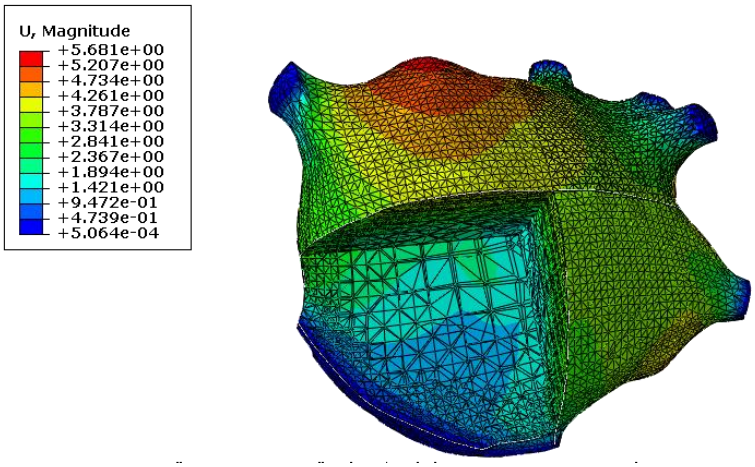

Figure I.55. Displacements obtained with 1000 nN/µm of focal adhesion stiffness.

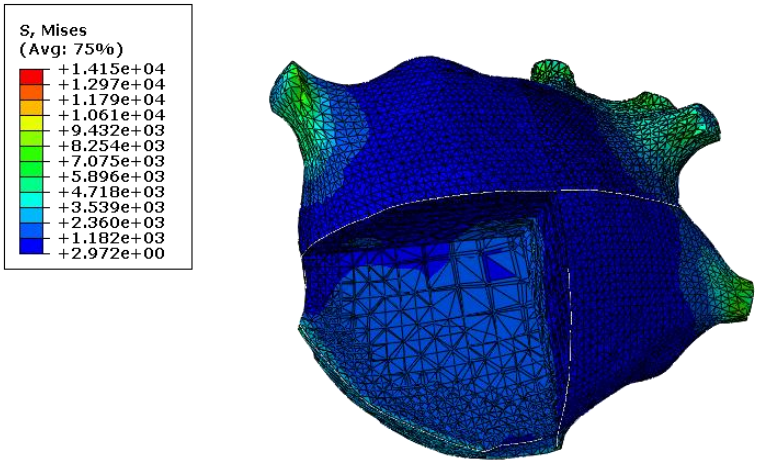

Figure I.56. Stresses obtained with 1000 nN/µm of focal adhesion stiffness.

It can be observed that as the stiffness of the adhesion increases, the displacements of the whole cell and the stresses in the focal adhesions increase. On the other hand, the displacement of the focal adhesions decreases as the stiffness increases. To summarize

this behaviour, the figure I.57 is showed. There, it can be seen the same behaviour than in the cell without nucleus in which both displacements reach a plateau.

Nevertheless, the maximum displacement of the cell obtains a lower value compared with the cell without nucleus. This fact can be explained because the cell has less active volume inside and cannot exert the same force as the previous case.

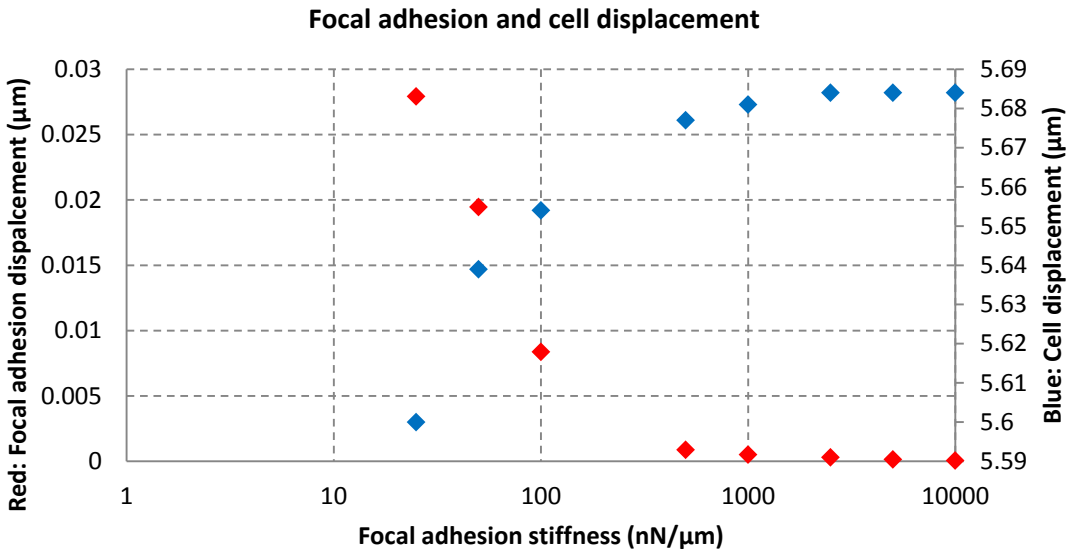

Figure I.57. Focal adhesion displacement (red) and cell displacement (blue) depending on the stiffness of the substrate.

The cellular response in terms of stress is similar to the previous section, where the stress reaches a maximum value around 14.5 kPa when the stiffness of the focal adhesion reaches 500 nN/ µm.

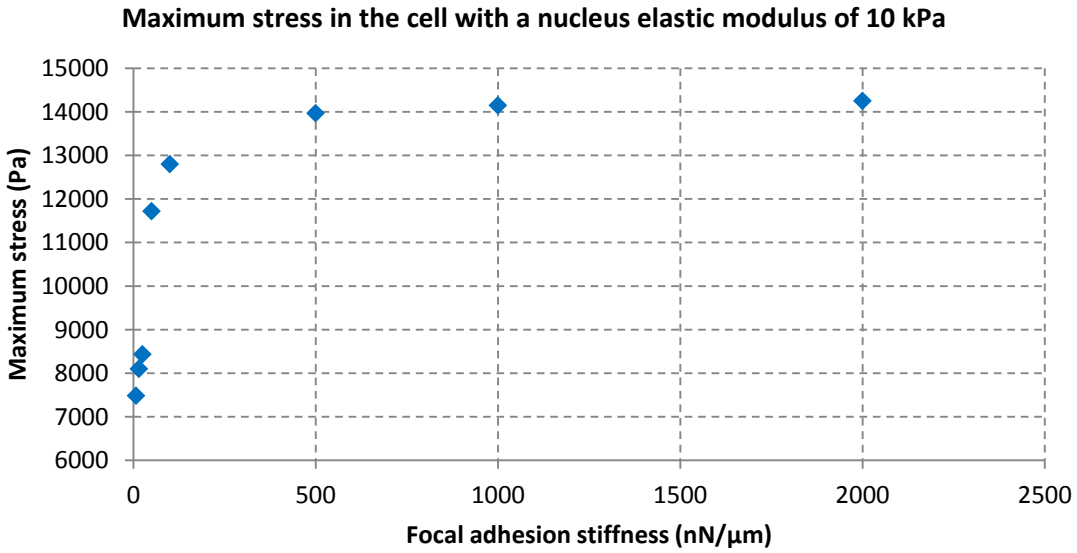

Figure I.58. Maximum stress obtained within the cell with nucleus depending on the stiffness of the simulated adhesions. The elastic modulus of the nucleus is set to 10 kPa.

b) Cell nucleus with an elastic modulus of 100 kPa.

Following, the elastic modulus is increased to 100 kPa. In the same way as the previous section, three main results are showed below with three cutting planes that allow seeing inside the cell to observe the nucleus behaviour.

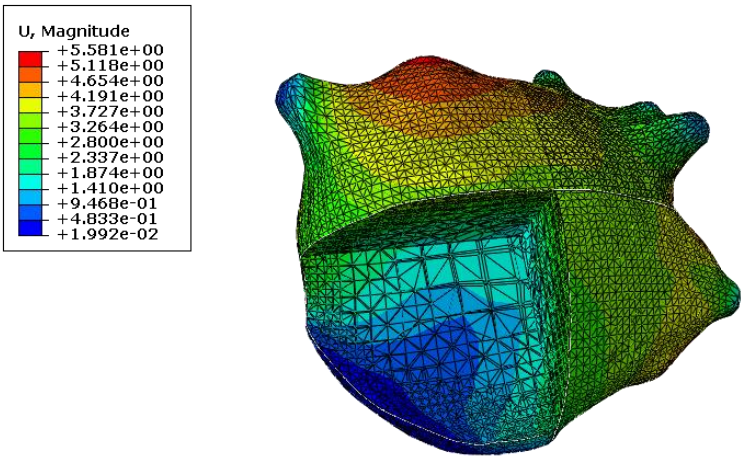

Figure I.59. Displacements obtained with 7.5 nN/µm of focal adhesion stiffness.

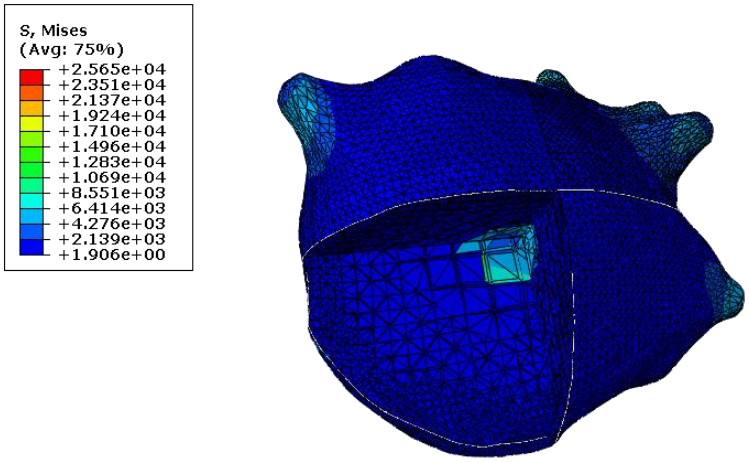

Figure I.60. Stresses obtained with 7.5 nN/µm of focal adhesion stiffness.

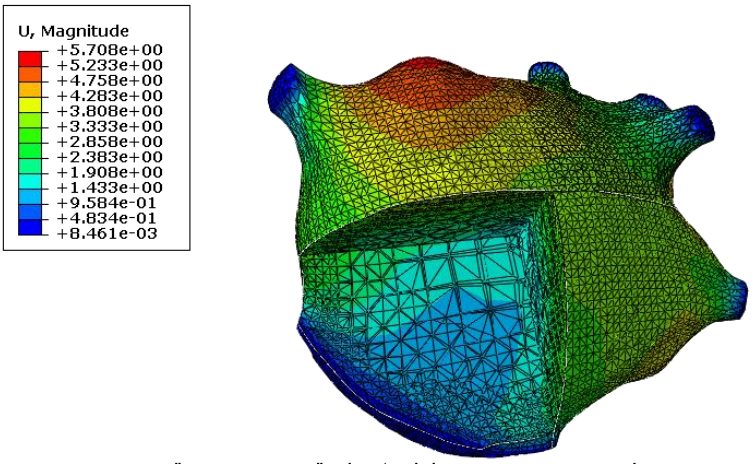

Figure I.61. Displacements obtained with 100 nN/µm of focal adhesion stiffness.

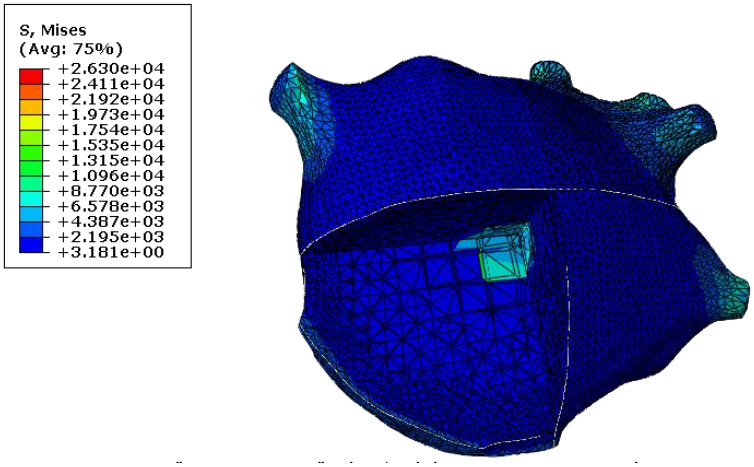

Figure I.62. Stresses obtained with 100 nN/µm of focal adhesion stiffness.

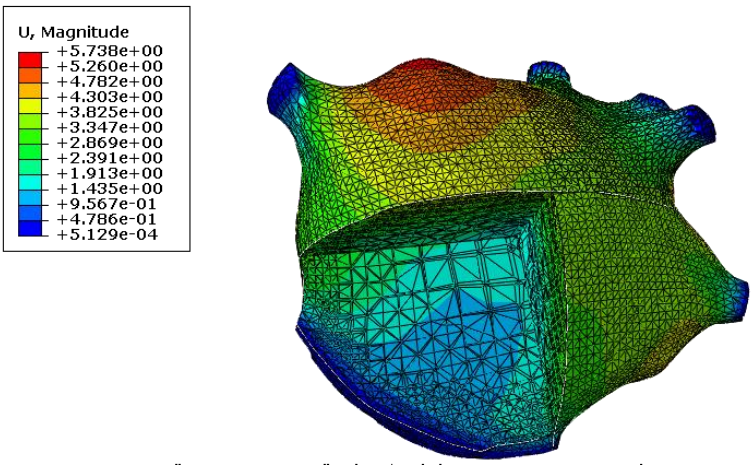

Figure I.63. Displacements obtained with 1000 nN/µm of focal adhesion stiffness.

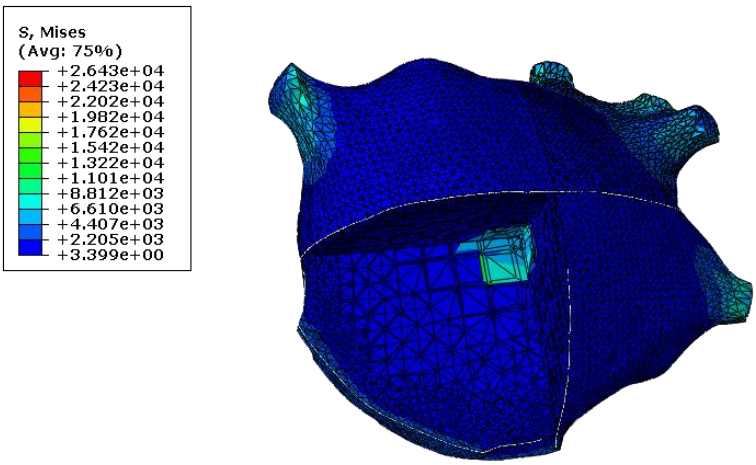

Figure I.64. Stresses obtained with 1000 nN/µm of focal adhesion stiffness.

The main difference that can be found between both models with nucleus is the solicitation of this part. In the second case, the nucleus is stiffer and hence, dissimilarities can be found in the stress field.

Attending to focal adhesions and cell displacements, there is little difference between them. However, as can be seen in figure I.65, less displacement is achieved by this later model.

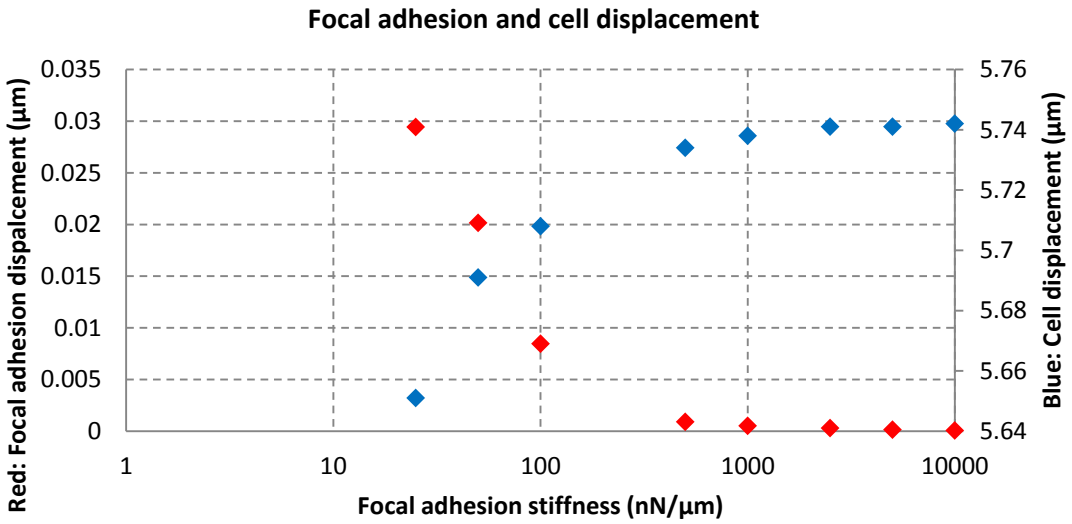

Figure I.65. Focal adhesion displacement (red) and cell displacement (blue) depending on the stiffness of the substrate.

It is remarkable that the displacement of the focal adhesions and the cell with lower stiffnesses are greater than the cases above. This behaviour can be explained because the nucleus is stiffer than the previous case and not only feels the stiffness of the focal adhesions but also the stiffness of its nucleus. In this way, the cell exerts more force and increases its displacements.

Nevertheless, the stress generated in the cell is similar to the previous cases as can be seen in figure I.66 The stress reaches a maximum value around 14.5 kPa when the stiffness of the focal adhesion reaches 500 nN/ µm.

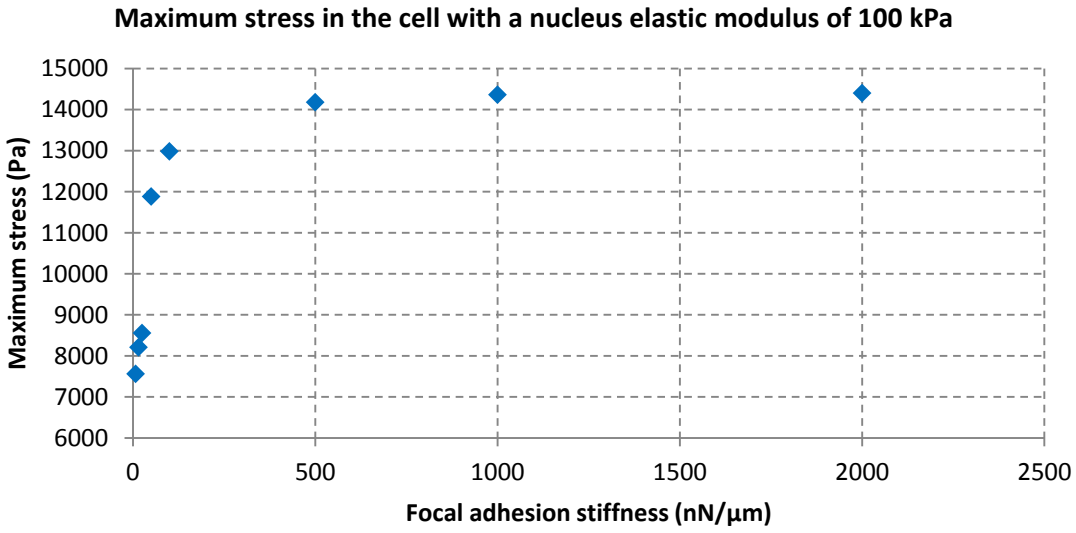

Figure I.66. Maximum stress obtained within the cell with nucleus depending on the stiffness of the simulated adhesions. The elastic modulus of the nucleus is set to 100 kPa.

Universidad Zaragoza
1542

Cellular response due to substrate stiffness variations: A phenomenological model

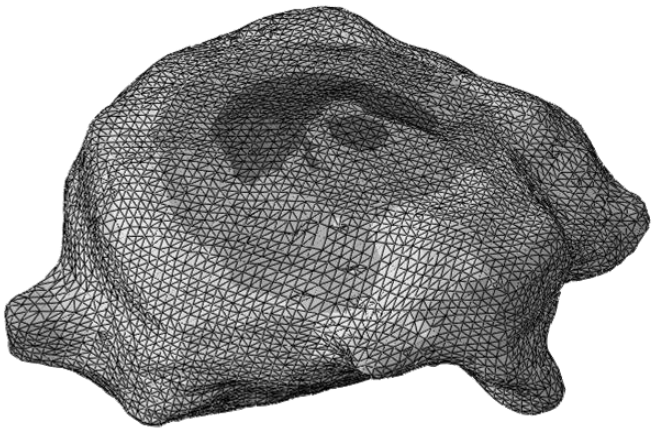

Appendix II – Programming codes

Appendix II – Programing codes

1. Introduction.

In this appendix is shown the main programming codes employed for the model development that comprises three codes: The phenomenological model, the element duplication subroutine and the substrate deletion and nucleus creation.

2. The phenomenological model.

The phenomenological model is programmed as combination of user subroutines in Abaqus® and then compiled with Intel® Fortran Compiler. The code, with comments, is exposed below.

```
C Variables to be defined.

      MODULE GLOBVAR
      PARAMETER (NELEMS=6243)
      PARAMETER (NNODES=2736)
      PARAMETER (NPGAUSS=8)
      REAL*8 EMIN(NELEMS,NPGAUSS)
      REAL*8 EAVE(NELEMS,NPGAUSS)
      REAL*8 EMAX(NELEMS,NPGAUSS)
      REAL*8 EXPANS_ELE(NELEMS,3)
      REAL*8 EXPANS_LAST(NELEMS,3)
      REAL*8 EcompMAX
      REAL*8 EcompAVE
      REAL*8 EcompMIN
      END MODULE

C ------------------------UEXTERNALDB-------------------------------C
C It allows to work with several subroutines.                       C
C-------------------------------------------------------------------C

      SUBROUTINE UEXTERNALDB(LOP,LRESTART,TIME,DTIME,KSTEP,KINC)

      USE GLOBVAR
      INCLUDE 'ABA_PARAM.INC'

      DIMENSION TIME(2)
        CHARACTER(256) FILENAME
        CHARACTER(256) JOBDIR

      if (LOP.EQ.0) then

C LOP 0: the subroutine is called at the start of the analysis.
C Values are set to 0.

      EMIN=0.0d0
      EAVE=0.0d0
      EMAX=0.0d0
      EXPANS_ELE=0.0d0
      EXPANS_LAST=0.0d0

      endif

      if (LOP.EQ.1) then
```

```
C LOP 1: the subroutine is called at the start of the increment.
       call GETOUTDIR(JOBDIR,LENJOBDIR)

      endif

      if (LOP.EQ.2) then

C LOP 2: the subroutine is called at the end of the increment.

        EXPANS_ELE=EXPANS_LAST

      endif

      if (LOP.EQ.3) then

C LOP 3: the subroutine iss called at the end of the analysis.

      close(101)

      endif

      RETURN
      END

C ------------------------------URDFIL---------------------------------C
C It allows to read the result files.                                   C
C----------------------------------------------------------------------C

      SUBROUTINE URDFIL(LSTOP,LOVRWRT,KSTEP,KINC,DTIME,TIME)

      USE GLOBVAR
      INCLUDE 'ABA_PARAM.INC'

      DIMENSION ARRAY(6000),JRRAY(NPRECD,6000),TIME(2)
      EQUIVALENCE(ARRAY(1),JRRAY(1,1))

      integer KELEM,KPOINT

      CALL POSFIL(KSTEP,KINC,ARRAY,JRCD)

      DO K1=1,999999999
            CALL DBFILE(0,ARRAY,JRCD)
                  IF (JRCD.NE.0) GO TO 110
               KEY=JRRAY(1,2)
               IF (KEY.EQ.1) THEN

C KELEM, element number (Record key 1, record type 1 y 2 + 2, to
define JRRAY(1,1).
C KPOINT, integration point.

                     KELEM=JRRAY(1,3)
                     KPOINT=JRRAY(1,4)
               ENDIF

C Record KEY 21: Total strain. First, second, etc.
C Record KEY 403: Principal strains en orden: MIN, MID, MAX.

               IF (KEY.EQ.21) THEN
                   EMIN(KELEM,KPOINT)=ARRAY(3)
                   EAVE(KELEM,KPOINT)=ARRAY(4)
                   EMAX(KELEM,KPOINT)=ARRAY(5)
                   write(101,*),EMAX(KELEM,KPOINT),EAVE(KELEM,KPOINT),
```

```
     * EMIN(KELEM,KPOINT)
            ENDIF

       ENDDO

  110  CONTINUE
       return
       end

C-----------------------------UEXPAN---------------------------------C
C It calculates the element expansion.                               C
C--------------------------------------------------------------------C

        SUBROUTINE UEXPAN(EXPAN,DEXPANDT,TEMP,TIME,DTIME,PREDEF,
      1 DPRED,STATEV,CMNAME,NSTATV,NOEL)

       USE GLOBVAR
       INCLUDE 'ABA_PARAM.INC'

       CHARACTER*80 CMNAME
       REAL*8 KACT, FMAX, KPAS, INFLIM, SUPLIM, EMAXX, ALPHA(3)
       REAL*8 TOLERANCIA

       DIMENSION EXPAN(*),DEXPANDT(*),TEMP(2),TIME(2),PREDEF(*),
      1 DPRED(*),STATEV(NSTATV)

C KACT: Actin stiffness.
C KPAS: Passive stiffness.
C FMAX: Maximum force of the contractil system.
C INFLIM: Upper strain limit.
C SUPLIM: Lower strain limit.

        KACT=10000.0d0
        FMAX=2500.0d0
        INFLIM=-0.4d0
        SUPLIM=0.4d0
        LIM=FMAX/KACT

C Average of the Gauus point in each element for EMAX, EAVE, EMIN.

        EcompMAX=SUM(EMAX(NOEL,:))/NPGAUSS
        EcompAVE=SUM(EAVE(NOEL,:))/NPGAUSS
        EcompMIN=SUM(EMIN(NOEL,:))/NPGAUSS

C EXPAN(1): X, EXPAN(2): Y, EXPAN(3): Z

C-----------------EMAX -----------------C

        IF (EcompMAX .LT. INFLIM)THEN

C The strain of the last step is read, that is the total strain.
C The new expansion increment will be ALPHA minus the last strain
state.

        ALPHA(2)= EcompMAX
        EXPAN(2)= ALPHA(2)- EXPANS_ELE(NOEL,2)

        ELSE IF ((EcompMAX .GE. INFLIM) .AND. (EcompMAX .LE. LIM))THEN

C Alpha is calculated (total strain) as function of the last strain
state.
```

```
        ALPHA(2)= ((EcompMAX-(FMAX/KACT))*INFLIM*KACT)/(KACT*INFLIM-
FMAX)

C The new value for the strain increment is de previously calculated
minus the element strain value of the previous state.

        EXPAN(2)= ALPHA(2)- EXPANS_ELE(NOEL,2)

        ELSE IF ((EcompMAX .GT. LIM) .AND. (EcompMAX .LE. SUPLIM)) THEN

        ALPHA(2)= ((EcompMAX-(FMAX/KACT))*SUPLIM*KACT)/(KACT*SUPLIM-
FMAX)
        EXPAN(2)= ALPHA(2)- EXPANS_ELE(NOEL,2)

        ELSE IF (EcompMAX .GT. SUPLIM)THEN

        ALPHA(2)= EcompMAX
        EXPAN(2)= ALPHA(2)- EXPANS_ELE(NOEL,2)

        END IF

C-----------------EAVE-----------------C

        IF (EcompAVE .LT. INFLIM)THEN

        ALPHA(1)= EcompAVE
        EXPAN(1)= ALPHA(1)- EXPANS_ELE(NOEL,1)

        ELSE IF ((EcompAVE .GE. INFLIM) .AND. (EcompAVE .LE. LIM))THEN

        ALPHA(1)= ((EcompAVE-(FMAX/KACT))*INFLIM*KACT)/(KACT*INFLIM-
FMAX)
        EXPAN(1)= ALPHA(1)- EXPANS_ELE(NOEL,1)

        ELSE IF ((EcompAVE .GT. LIM) .AND. (EcompAVE .LE. SUPLIM)) THEN

        ALPHA(1)= ((EcompAVE-(FMAX/KACT))*SUPLIM*KACT)/(KACT*SUPLIM-
FMAX)
        EXPAN(1)= ALPHA(1)- EXPANS_ELE(NOEL,1)

        ELSE IF (EcompAVE .GT. SUPLIM)THEN

        ALPHA(1)= EcompAVE
        EXPAN(1)= ALPHA(1)- EXPANS_ELE(NOEL,1)

        END IF

C-----------------EMIN-----------------C

        IF (EcompMIN .LT. INFLIM)THEN

        ALPHA(3)= EcompMIN
        EXPAN(3)= ALPHA(3)- EXPANS_ELE(NOEL,3)

        ELSE IF ((EcompMIN .GE. INFLIM) .AND. (EcompMIN .LE. LIM))THEN

        ALPHA(3)= ((EcompMIN-(FMAX/KACT))*INFLIM*KACT)/(KACT*INFLIM-
FMAX)
        EXPAN(3)= ALPHA(3)- EXPANS_ELE(NOEL,3)

        ELSE IF ((EcompMIN .GT. LIM) .AND. (EcompMIN .LE. SUPLIM)) THEN
```

```
        ALPHA(3)= ((EcompMIN-(FMAX/KACT))*SUPLIM*KACT)/(KACT*SUPLIM-
FMAX)
        EXPAN(3)= ALPHA(3)- EXPANS_ELE(NOEL,3)

        ELSE IF (EcompMIN .GT. SUPLIM)THEN

        ALPHA(3)= EcompMIN
        EXPAN(3)= ALPHA(3)- EXPANS_ELE(NOEL,3)

        END IF

        EXPANS_LAST(NOEL,1)=ALPHA(1)
        EXPANS_LAST(NOEL,2)=ALPHA(2)
        EXPANS_LAST(NOEL,3)=ALPHA(3)

       RETURN
       END
```

3. Element duplication.

As previously exposed, the model is based on a set of duplicated elements. Nevertheless, depending on the design, the number of elements to be duplicated can be unapproachable, so a Matlab® subroutine is created to facilitate the addition of the duplicated elements. The program is exposed below.

```
clear all

load Elset.txt;

[Elem, Nodes] = size(Elset);

% Elem (rows): Set element number.
% Nodos (columns): Node number +1, corresponding to element number.

for i=1:1:Elem
    for j=1:1:Nodes
        if j==1;
        Add(i,j)=Elem;
        else
        Add(i,j)=0;
        end
    end
end

% First column stores the last element number of the set.
% Rest of the columns correspond to the node position of that element
% and are set to 0 to avoid modifications in the element shape.

% Generated matrix is added to Elset matrix. This way, the elements
% are duplicated avoiding node modification.

NewElset=Elset+Add;

fid=fopen('Elem_Hex.txt','w');
fprintf(fid,'%2d, %2d, %2d, %2d, %2d, %2d, %2d, %2d, %2d \n',
NewElset');
fclose(fid);
```

4. Substrate deletion and nucleus creation.

To make the deletion of the substrate is needed a program to eliminate all elements that are not included in the cell. Additionally, to create the nucleus, the cell centroid must be calculated and then, taking it as reference, it is described a sphere of a given radius. All elements within the sphere will form the nucleus while the elements outside will make up the cytoskeleton.

```
clear all
clc

% Load files

nodes_raw=load('Nodos.txt');
conec_raw=load('Conectividad.txt');

nelem=size(conec_raw,1);

conec=[conec_raw(:,2) conec_raw(:,3) conec_raw(:,4) conec_raw(:,5)];
node_list=[conec_raw(:,2); conec_raw(:,3); conec_raw(:,4);
conec_raw(:,5)];
node_list=sort(node_list); %Sort the list
node_list=unique(node_list); %Delete duplicated nodes

nodes_coord=nodes_raw(node_list,:);

nnodes=size(nodes_coord,1); %Final number of nodes

conec_final=conec;
c=0;

for n=1:nnodes
   c=c+1;

   temp_index=nodes_coord(n,1); %the index from the orginal mesh
   nodes_coord(n,1)=c; %the new index

   k=find(conec==temp_index);%Find all the nodes numbered as
temp_index
   conec_final(k)=c; %Change them to the new index

   if mod(c,1000)==0
       fprintf('%d nodes from %d processed (~%2.2f%%)...
\n',c,nnodes,c/nnodes*100);
   end

end

fprintf('---------------------- \n');
fprintf('Printing new files... \n');
fi=fopen('New_coords.txt','w');
fprintf(fi,'%d , %3.6f , %3.6f , %3.6f  \n',nodes_coord');
fclose(fi);

conec_final=[(1:nelem)' conec_final];

fi=fopen('New_conec.txt','w');
```

```
fprintf(fi,'%6d , %6d , %6d , %6d, %6d  \n',conec_final');
fclose(fi);

fprintf('---------------------- \n');
fprintf('Calculating nucleus... \n');

elem_centroids=zeros(nelem,3);

temp_cent=[0 0 0];
% Calculate centroid of each element
for n=1:nelem

    for k=1:4
      k_node=conec_final(n,k+1);
      temp_cent=temp_cent+[nodes_coord(k_node,2) nodes_coord(k_node,3)
nodes_coord(k_node,4)];
    end

    elem_centroids(n,:)=temp_cent/4; %Centroid of the element n

    temp_cent=[0 0 0];
end

% Calculate cell centroid

cell_centroid=sum(elem_centroids)/nelem ;

% Calculate list of elements within a sphere of a specific radius (the
nucleus)

list_nucleus=zeros(nelem,1);
radius=5

for n=1:nelem

    dist=norm(cell_centroid-elem_centroids(n,:));
    if dist<radius
        list_nucleus(n,1)=n;
    end

    if dist>=radius
        list_cyto(n,1)=n;
    end

end

list_nucleus=list_nucleus(list_nucleus~=0); %Clear the zeros

fprintf('---------------------- \n');
fprintf('Printing nucleus... \n');
fi=fopen('Nucleus.txt','w');
fprintf(fi,'%5d , %5d, %5d, %5d, %5d, %5d, %5d, %5d,
\n',list_nucleus);
fclose(fi);

fprintf('---------------------- \n');
fprintf('Printing cytoskeleton... \n');
fi=fopen('Cytoskeleton.txt','w');
```

```
fprintf(fi,'%5d , %5d, %5d, %5d, %5d, %5d, %5d, %5d, \n',list_cyto);
fclose(fi);

fprintf('DONE!! \n');
```

Universidad Zaragoza
1542

Cellular response due to substrate stiffness variations: A phenomenological model

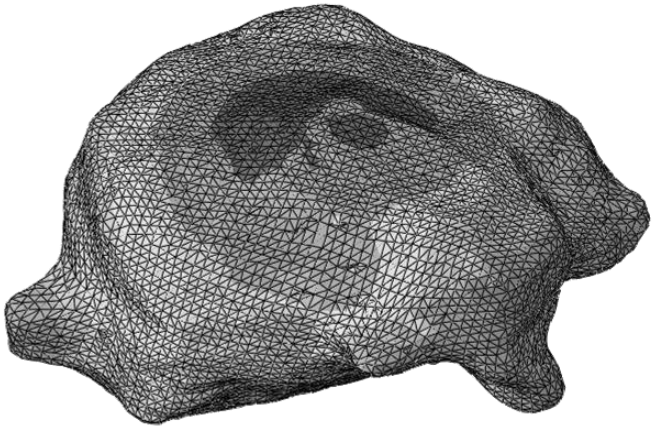

Appendix III – Glossary

Appendix III - Glossary

Lamellipodium.

Sheetlike extensions of cytoplasm that form transient adhesions with the cell substrate and wave gently, enabling the cell to move along the substrate.

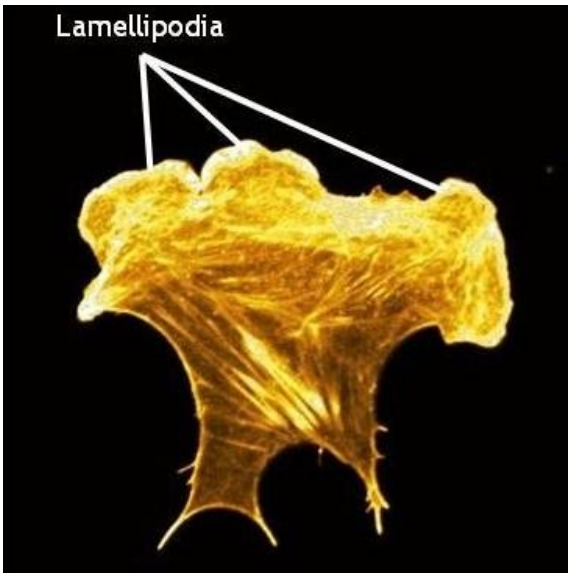

Figure III.1. Lamellipodia in a cell stained for F-actin. Wei Wei Luo, Mechanobiology Institute, Singapore.

Filopodia.

The filopodia are slender cytoplasmic projections, which extend from the leading edge of migrating cells. They contain actin filaments cross-linked into bundles by actin-binding proteins. Filopodia form focal adhesions with the substratum, linking it to the cell surface.

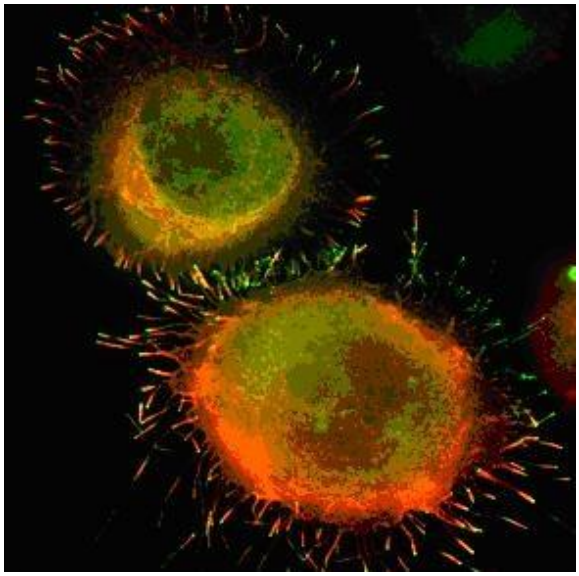

Figure III.2. Filopodia of macrophages, Mechanobiology Institute, Singapore.

Extracellular matrix.

A substantial part of tissue volume is the extracellular space, filled by an intricate network of macromolecules constituting the extracellular matrix. This matrix is composed of a variety of proteins and polysaccharides that are secreted locally and assembled into an organized mesh in association with the cells that produced them. Extracellular matrix concentrates on connective tissues and determines the physical properties of the tissue.

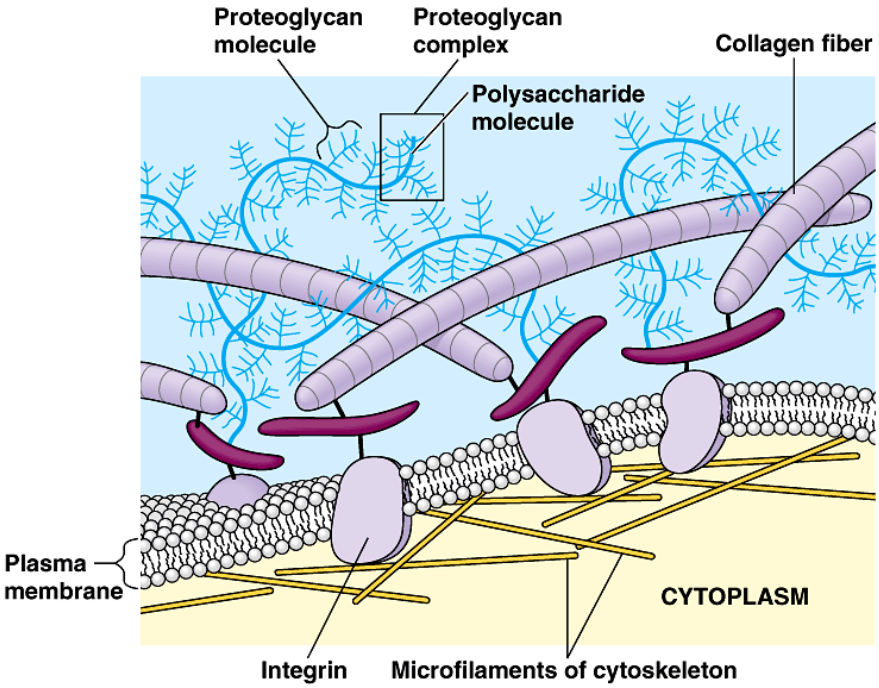

Figure III.3. Extracellular matrix. Pearson Education, Inc.

Fibronectin.

Fibronectin is a high-molecular weight glycoprotein of the extracellular matrix that binds to the integrins, the membrane receptor proteins. Similar to integrins, fibronectin binds extracellular matrix components such as collagen, fibrin, and proteoglycans. Fibronectin exists as a protein dimer, consisting of two nearly identical monomers linked by a pair of disulfide bonds.

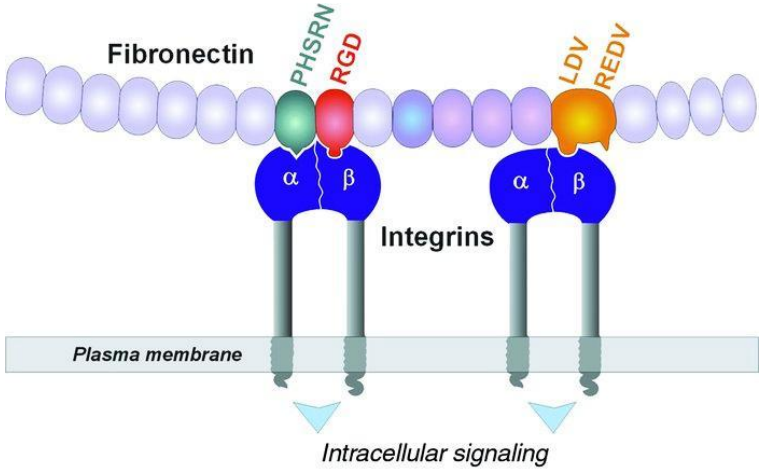

Figure III.4. Relationship between integrin and fibronectin. Seehint, 2011.

Integrin.

Integrins are transmembrane receptors that mediate the attachment between a cell and its surroundings, such as other cells or the extracellular matrix. In signal transduction, integrins pass information about the chemical composition and mechanical status of the ECM into the cell. Therefore, they are involved in cell signalling and the regulation of cell cycle, shape, and motility.

Focal adhesion.

Adhesion complexes are dynamic structures and are constantly being assembled and disassembled in actively migrating cells. Focal adhesions are large, stable complexes composed of large numbers of proteins to increase adhesion and therefore reduced cell migration. Integrins bind to components of the extracellular matrix such as collagen and fibronectin. The integrins are linked to the actin cytoskeleton and this interaction is established by the binding of proteins such as talin, tensin and vinculin. As the cell continues to move forward this complex of proteins dissociates, allowing the cell to detach from the extracellular matrix and re-attach at another point.

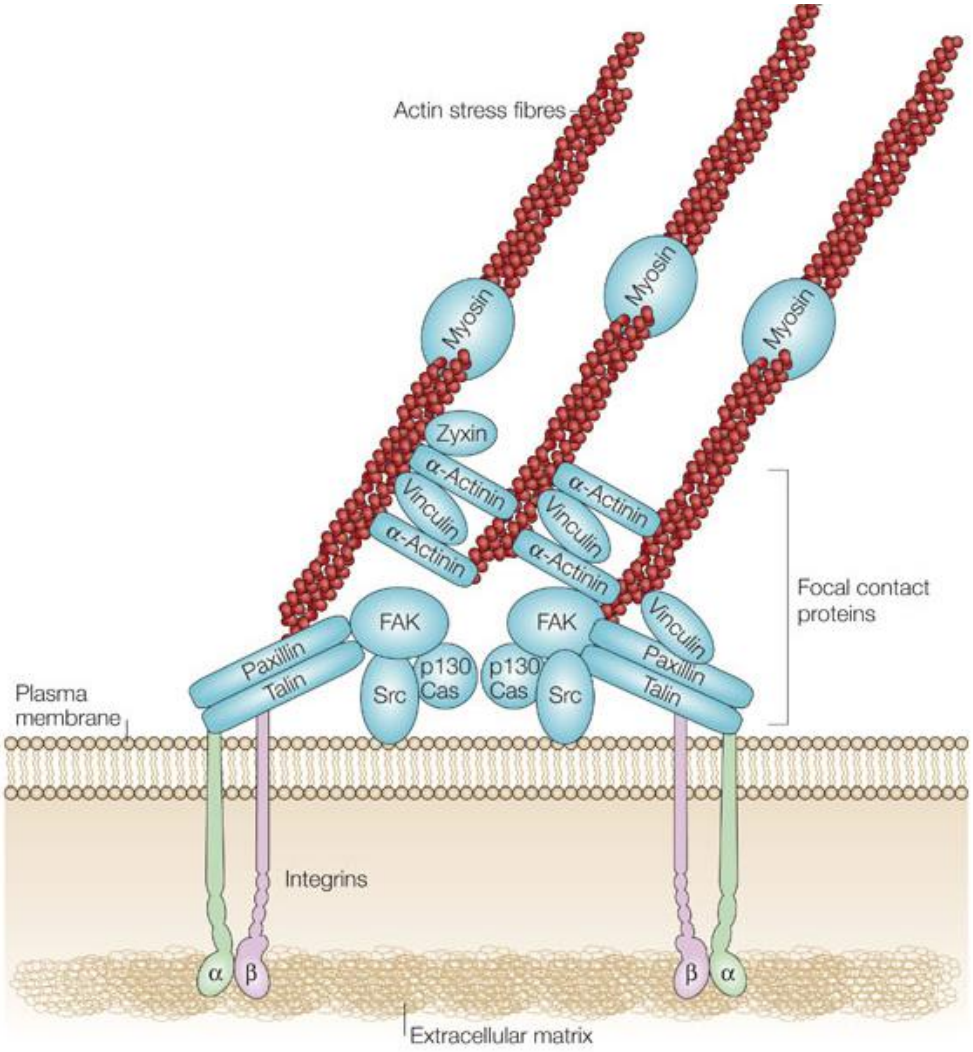

Figure III.5. Focal adhesion and acto-myosin complex contraction. Nature reviews. Molecular Cell Biology.

Acto-myosin complex.

Actin and myosin complex leads cell contraction and motility. For its part, actin is a globular protein that forms microfilaments, present as a free monomer, called G-actin, or as part of a linear polymer microfilament, called F-actin. On the other hand, the myosin is an ATP-dependent motor protein and is responsible for actin-based motility by mean of ATP hydrolysis. They can be found in all eukaryotic cells.